Pak. J. Chem. 16(1-2):45-64, 2026 Research article
ISSN (Print): 2220-2625
ISSN (Online): 2222-307X DOI: 10.15228/2026.v16.i1-2.p06

Designing, Synthesis, Characterization, and In Vitro Antibacterial Evaluation of Novel Nicotinamide-Derived Schiff Bases as Potential Therapeutic Agents

Muhammad Javid[1], Muhammad Asad Masood[2], Farah Yaqoob[3], Muhammad Sagheer[1], Muhammad Sajid Abbas[2], Muhammad Hasnain[1], Ihsan Maseeh[4], Sabahat Asghar[5]
[1]Department of Chemistry, University of Agriculture, Faisalabad 38000, Pakistan.
[2]Department of Physics, University of Agriculture, Faisalabad 38000, Pakistan.
[3]Department of Zoology, The Islamia University of Bahawalpur 63100, Pakistan.
[4]Institute of Chemistry, The Islamia University of Bahawalpur 63100, Pakistan.
[5]Institute of Chemistry, Khwaja Fareed University of Engineering & Information Technology, Rahim Yar Khan, Pakistan.
***Corresponding Author email**: javidkhanchemist@gmail.com

Abstract
The growing bacterial resistance to currently used antibiotics emphasizes the need to explore novel substances with efficacy against harmful microorganisms. Despite the availability of diverse classes of disinfectant agents, the development of drug resistance among pathogenic bacteria remains a current issue. The wide array of chemical structures and mechanisms of action further complicates the goal for a definitive approach to discovering new pharmaceuticals. The requirement to manufacture newly discovered drugs is condemnatory, as contagious microorganisms can spread swiftly throughout the body and cause ailments such as epidemic cholera, *Salmonella typhi* infection, pleurisy, and plague. The search for novel, targeted, and safe antibacterial agents has emerged as a pivotal area of research in organic chemistry. In this research study, nicotinamide and different benzaldehydes were condensed to produce a series of Schiff bases. Nicotinamidium products are of significant importance and find utility across various fields due to their distinct properties. The synthesized compound was thoroughly distinguished by UV-vis, FTIR, and NMR (^{1}H-NMR & ^{13}CNMR spectroscopy). Antimicrobial activities were tested against bacteria (*E. coli and S. aureus*) using the disc diffusion method, with ciprofloxacin as the standard. According to the data, the product demonstrated significant antibacterial activity against the tested bacterial strains. To evaluate the antioxidant potential, the DPPH radical scavenging assay was employed. The antioxidant applications demonstrated moderate inhibition of oxidation.

Keywords: Schiff base, Nicotinamide Synthesis, Antimicrobial, Antioxidant, Spectroscopy,

1. Introduction
Recently, antibacterial resistance has been increasing gradually due to its significance and indispensability in several fields, such as medical science, personal hygiene, and sanatoriums [1]. A prevalent sickness condition that has afflicted humans for a long time is bacterial infection. As a result of the lack of antibiotics, sepsis from small wounds and commonplace infections were among the fatalities that occurred about a century ago, and having a bacterial infection was considered a death sentence [2]. Antibiotics saved millions of lives globally and transformed the provision of Healthcare [3]. Unfortunately, the misuse of antibiotics has led to the emergence of multidrug-resistant bacteria [4]. Consequently, a multifaceted approach is required to combat this situation [5]. One method of treating bacterial infections is the use of Schiff bases and their complexes [6]. The condensation of ketones or aldehydes with primary amines yields a class of compounds known as Schiff bases [7]. They have a functional group called azomethine, which is related to an alkyl or aryl group but not to hydrogen [8]. It has a carbon-nitrogen double bond (>C=N–) [9]. The broad range of biological and pharmacological properties of Schiff base compounds and their complexes, along with their applications in other fields of study, has drawn the attention of researchers [10]. According to reports, Schiff base compounds exhibit a wide range of biological activities, including antitumor, antifungal, antibacterial, and anti-inflammatory effects [11]. The bioactive core of Schiff bases is the azomethine or imine (>C=N–) moiety, which plays a key role in disinfection, analytical applications, magnetism, free-radical scavenging, antimycotic, biochemical reactions, and bioorganometallic modeling [12]. By removing crimps, nicotinamide can retard skin aging [13]. Other names for nicotinamide include vitamin B3, nicotinic acid amide, and niacin [14]. Nicotinamide is a vital component of N-donor ligand systems in heterocyclic compounds [15]. Nicotinamide is a bioligand having a chemical formula $C_6H_6N_2O$ [16]. It is used in the treatment of pellagra, anorexia nervosa and hypercholesteremia diseases [17-21].

It is advantageous to synthesize several Schiff bases and investigate their biological behavior by condensation of nicotinamide derivatives with various aldehydes, such as furfuraldehyde, thiophene-2-carboxaldehyde, 5-bromosalicylaldehyde, 5-bromo-2-hydroxybenzaldehyde, 2-hydroxy-5-nitrobenzaldehyde, 2-hydroxy-5-methoxybenzaldehyde, and 5-bromosalicylaldehyde [18]. This exploration may lead to the discovery of new targets to combat strains of bacteria and fungi that have become resistant to some currently available and widely used antimicrobial agents [19]. Zone of inhibition studies showed that Schiff bases were more active against bacteria than Ampiclox and against fungi than ketoconazole [20]. The most vulnerable bacteria were *P aeruginosa*, *Bacillus subtilis*, *Escherichia coli*, and *Enterobacter aerogenes* [21].

A study used 5-methoxysalicylaldehyde and nicotinamide derivatives to produce numerous Schiff bases, which were spectroscopically characterized by FTIR, 1H-NMR, 13C-NMR, and UV spectroscopy [22]. To determine the synthesized products' possible antibacterial activity, they were tested against several bacteria using ampicillin as a reference (ampicillin) [23]. Except for the *Candida albicans* isolate, which showed a 0-mm zone of inhibition, the Schiff base showed antibacterial activity against all examined microorganisms [24].

Humanity is seriously threatened by antibiotic resistance in microorganisms; hence, it is imperative to investigate a wide range of potential drug candidates for their antimicrobial and antibiotic activities [25]. The new Schiff base, derived from nicotinamide with o-aminobenzaldehyde [26]. The antibacterial activity of the prepared Schiff base was screened against several bacterial strains, including *S. aureus*, *E. coli*, *Proteus mirabilis*, and *P. aeruginosa* [27]. According to the findings of Sabt et al., [28], the Schiff base was also more effective in antimicrobial activity screening than standard drugs against the majority of the test bacterial isolates; however, *S. aureus* and *P. aeruginosa* bacterial isolates were not susceptible to the effects of nicotinamide imines

Wang et al. [29] in their research work established the formation of a new class of chemical compounds that combine the advantages of both nicotinamide and a conjugated π-spacer, i.e., C=N. Preparation of a new class of Schiff base based on nicotinamide will display enhanced properties and add new structural units to the list of Schiff bases [29]. The presence of nicotinamide and various aldehydes, along with the conjugated pi-bond, can be beneficial for producing moieties with improved performance in antibacterial, antifungal, antioxidant, anti-inflammatory, and antimalarial applications [30]. Moreover, conjugated nicotinamide-based Schiff bases are affordable and easy to synthesize [31].

The aims and objectives of the current research are a synthesis of a series of novel conjugated imines through the reflux process of nicotinamide or nicotinamide-based derivatives with different aldehydes like Vanillin, 4-chlorobenzaldehyde, N, N-dimethyl amino benzaldehyde, 4-hydroxybenzaldehyde, 3-nitrobenzaldehyde, 3, 4-dimethoxybenzaldehyde, Cinnamaldehyde, 3-fluorobenzaldehyde, 2, 4-dichlorobenzaldehyde, salicylaldehyde, and crotonaldehyde. Antibacterial applications of Schiff bases were enhanced by their synthesis. The structures of Schiff base derivatives were validated using FTIR, UV-Vis, and ^{1}H-NMR spectroscopy, and their biological and antioxidant activities were also reported.

2.0. Materials and Methods

2.1 Substrates and Reagents

Nicotinamide, Vanillin, 4-Chlorobenzaldehyde, 2,4-Dichlorobenzaldehyde, 4-Hydroxybenzaldehyde, N, N-Dimethylaminobenzaldehyde, 3-Nitrobenzaldehyde, Cinnamaldehyde, 3-Fluorobenzaldehyde, 3,4-Dimethoxybenzaldehyde, and Salicylaldehyde were purchased from E. Merck and Sigma-Aldrich. Acetic acid, Ethanol, Methanol, DMSO, DMF, Ethyl acetate, Petroleum ether, n-hexane, Toluene, Tetrahydrofuran, H_2SO_4(conc.), DCM, chloroform, and distilled water were supplied by Lab Scan.

2.2 Instruments Used

A melting-point apparatus (Stuart SMP-10) was used to determine the melting point. A Bk-D560 Double Beam Spectrophotometer was used for UV-Vis. Spectra: Shimadzu IR-8400 was used for Infrared spectra. A Bruker spectrometer operating at 300 MHz was used for ^{1}H NMR spectra in CD_3OD solution. The internal reference standard was standard in this technique. Chemical shift values were measured in (ppm) by using the sigma scale. S, d, t, m, dd, and at, are abbreviations to show singlet, doublet, triplet, and multiplet, double doublet, and apparent triplet, respectively [32].

2.3 Antibacterial Activity

The antimicrobial activity of the newly synthesized nicotinamide-modified Schiff bases was evaluated using the disc diffusion method against *Staphylococcus aureus* and *Escherichia coli*. Prior to testing, bacterial isolates were cultured in nutrient broth and incubated for 18 hours at 37 °C until the turbidity reached the 0.5 McFarland standard (approximately 1×10^8 CFU/mL). The 0.5 McFarland standard was prepared by mixing 0.5 mL of 0.048 M $BaCl_2$ with 99.5 mL of 0.36 N H_2SO_4, resulting in a barium sulfate suspension. This turbidity standard was stored in a screw-capped test tube and used for comparison. Nutrient agar medium (2.3 g) was dissolved in 100 mL of distilled water, adjusted to pH 7.0, and sterilized by autoclaving. The medium was allowed to cool to approximately 45 °C before use. Sterile Petri plates were prepared by pouring the molten agar. The bacterial inoculum (adjusted to 0.5 McFarland standard) was evenly spread over the agar plates. Sterile discs impregnated with the test compounds (approximately 100 µg/mL) were placed on the inoculated agar surface. Control discs containing the corresponding solvents were included as negative controls, while penicillin (1 mg/mL) was used as a positive control. The plates were incubated at 37 °C for 24 hours, after which the zones of inhibition were measured in millimeters.

2.4. Antioxidant Activity (DPPH Assay)

The antioxidant activity of the synthesized compounds, namely N-(3,4-dimethoxybenzylidene) (solid), (E)-N-(4-chlorobenzylidene) nicotinamide, (E)-N-(3-nitrobenzylidene) nicotinamide, and N-(3,4-dimethoxybenzylidene) (liquid), was evaluated using the DPPH radical scavenging assay. A freshly prepared solution of DPPH (2,2-diphenyl-1-picrylhydrazyl) was prepared in methanol at a concentration of 0.004% (w/v). An aliquot of 1 mL of this DPPH solution was mixed with 3 mL of the test compound solution at various concentrations. The reaction mixtures were vortexed thoroughly and incubated in the dark at room temperature for 30 minutes to allow completion of the reaction. After

incubation, the absorbance of each sample was measured at 517 nm using a UV–visible spectrophotometer against methanol as a blank. A decrease in absorbance indicated the scavenging of DPPH free radicals by the test compounds. Ascorbic acid and butylated hydroxytoluene (BHT) were used as reference standard antioxidants for comparison. A control sample containing 1 mL of DPPH solution mixed with 3 mL of methanol (without test compound) was prepared. Additionally, a blank sample containing the test compound solution, but without DPPH, was used to correct for background absorbance. All experiments were performed in triplicate, and results were expressed as mean ± standard deviation. The concentration of the compound required to scavenge 50% of DPPH radicals (IC_{50}) was determined from the plot of percentage inhibition versus concentration. All experiments were performed in triplicate.

The percentage of the DPPH scavenging is calculated according to the following Equation:

$$\% \text{ inhibition of DPPH radical} = \frac{(\text{Acontrol} - \text{Asample})}{\text{Acontrol}} \times 100 \quad (1)$$

where $A_{control}$ is the absorbance of the control (before the reaction takes place) and A_{sample} is the absorbance after the reaction occurs.

2.5. Scheme of Study For the Synthesis of nicotinamide-based Schiff base derivatives

The designed compounds were synthesized by a conventional reaction between nicotinamide and various substituted benzaldehydes, using ethanol as the solvent, under acidic conditions to maintain the mixture at pH 3.5-4.5, and refluxing for 20 hours.TLC was used to check reaction progress. The mobile phase was ethyl acetate and petroleum ether in a 1:2 ratio. After reflux and stirring, this mixture cooled to room temperature and was left overnight. After cooling, precipitates were formed at the bottom of the flask. Then this solid product was filtered and dried. A small amount of the product formed at the bottom of the flask was added to distilled water. This solid product was filtered by using filter paper. Then cooled at the room temperature. The general scheme is given below where R= 3-methoxy-4-hdroxy, 3, 4-Dimethoxy, 4-chloro, 4-hydroxy, N, N-Dimethyl amino, 3-Nitro, 3-fluoro, 2, 4-dichloro. A series of nicotinamide-based imine byproducts were synthesized through a chemical process between nicotinamide and distinct aldehydes like Vanillin, 4-chlorobenzaldehyde, 2,4-dichlorobenzaldehyde, 3,4-dimethoxybenzaldehyde, N, N-dimethylamino benzaldehyde, 3-nitrobenzaldehyde, Cinnamaldehyde, 3-fluorobenzaldehyde, salicylaldehyde, crotonaldehyde, and 4-hydroxybenzaldehyde. Nicotinamide-based products have been synthesized by refluxing nicotinamide with various aldehydes in ethanol, with acetic acid or H_2SO_4, and characterized by UV-Vis, FTIR, ^1H NMR, and ^{13}C NMR techniques.

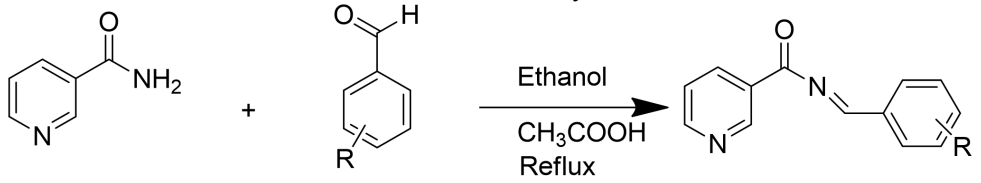

2.5.1. Synthesis of (E)-N-(3-hydroxy-2-methylbenzylidene) nicotinamide

Nicotinamide reacts with Vanillin using ethanol as solvent and conc. H_2SO_4 as a catalyst. The final product, N-(4-hydroxy-3-methoxybenzylidene) nicotinamide Schiff base, was synthesized by condensation. As a result, lemon-coloured precipitates formed. These precipitates were washed with ethanol and then filtered through filter paper. After washing, the colour of the precipitates changed from lemon to a shiny off-white. Off white shiny solid; % age Yield: 49%; Rf: 0.6; Melting point: 162-168°C; FTIR (U, cm^{-1}): 3073 (sp^2 CH stretch), 1645 (C=N stretch) 1608,1470 (C=C stretch); UV Vis (λ, nm): 315,342

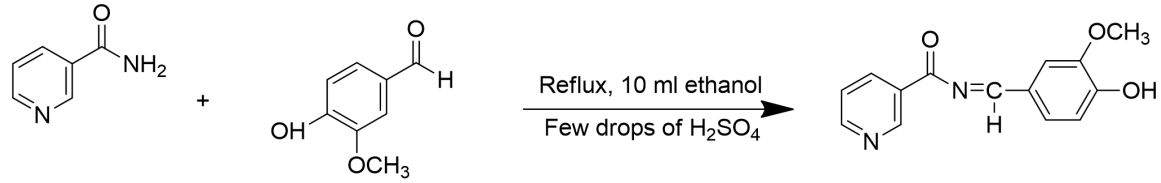

2.5.2. Synthesis of (E)-N-(3,4-dimethoxybenzylidene) nicotinamide

Nicotinamide reacts with 3, 4-dimethoxy benzaldehyde using C_2H_5OH as a dissolving agent, acetic acid as an agitator, while refluxing produces the final product N-(3-methoxy-4-methylbenzylidene) nicotinamide Schiff base by the process of condensation. After cooling, bright yellow precipitates were formed at the bottom of the flask was added to distilled water. As a result, pure yellow precipitates were formed. This solid product was filtered by using filter paper. Then cooled at the room temperature. Pure yellow solid; % age Yield: 9%; Rf: 0.57; M.P: >300°C; FTIR (U, cm^{-1}): 2935, 2830 (sp^3 CH stretch), 1522 (C=N stretch); UV Vis (λ, nm): 317,344

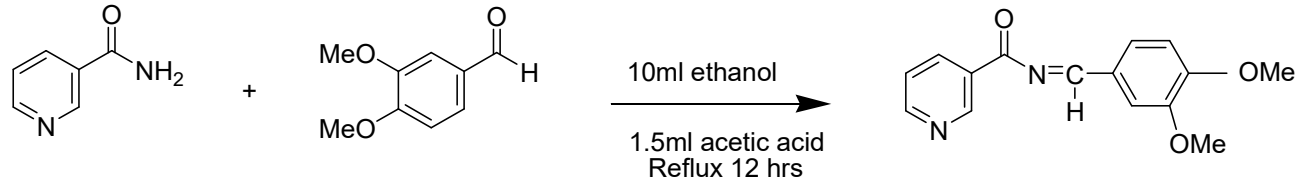

2.5.3. Synthesis of (E)-N-(4-chlorobenylidene) nicotinamide

Nicotinamide reacts with 4-chlorobenzaldehyde under reflux, producing the final product, N-(4-chlorobenylidene)nicotinamide Schiff base, by condensation. Consequently, a white crystalline product was appeared in the round-bottom flask. This product was filtered and dried. Inside the round-bottom flask, there were some particles of pure white crystalline product. To preserve these particles, 2 mL of cold distilled water was added to the flask. Precipitation of a white crystalline product occurred again, which was the original product. This crystalline white product was filtered and dried at room temperature. Crystalline whitish solid; % age Yield: 9%; Rf: 0.7; Melting point: 200-212°C; FTIR (U, cm^{-1}): 3073 (sp^2 CH stretch), 1695 (C=O), 1649 (C=N stretch); UV Vis (λ, nm): 342

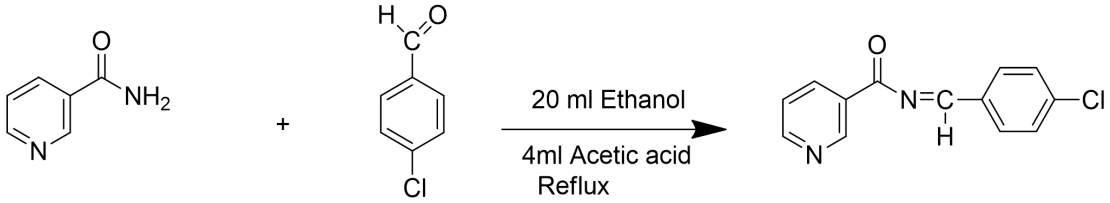

2.5.4. Synthesis of (E)-N-(2, 4-dichlorobenylidene) nicotinamide

N-(2,4-dichlorobenylidene)nicotinamide Schiff base was produced by refluxing a mixture of nicotinamide and 2,4-dichlorobenzaldehyde in ethanol, using acetic acid as a catalyst. The solvent from the resultant mixture was removed by rotary evaporation. After this, the obtained pure mixture was placed into a petri dish and allowed to cool and dry. The DCM was added to the cooled, dried mixture. Again, the drying of this mixture was carried out at room temperature and left overnight. As a result, a light greyish solid was formed; this product was properly scratched using a spatula. Light grey solid; % age Yield: 59%; Rf: 0.6; Melting point: 115-124°C; FTIR (U, cm^{-1}): 3088 (sp^2 CH stretch), 1589 (C=N stretch); UV Vis (λ, nm): 340, 334.

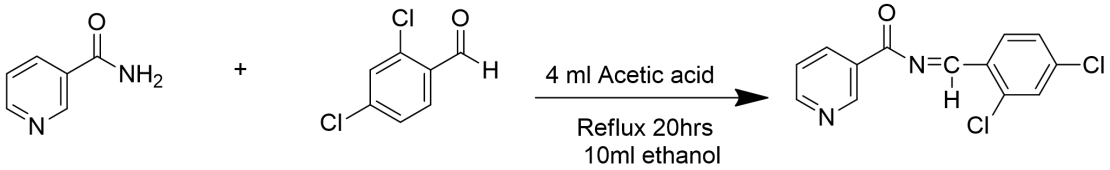

2.5.5. Synthesis of (E)-N-(4-hydroxybenylidene) nicotinamide

N-(4-hydroxybenzylidene) nicotinamide azomethines were synthesized by condensing p-hydroxybenzaldehyde with nicotinamide in ethanol, using H_2SO_4 as a catalyst under reflux. Then allowed to cool and dry. DCM was added to the admixture, which was cooled and dried. After this, a shiny off-white solid formed, which was scratched with a spatula. Shiny off white solid; % age Yield: 43%; Rf: 0.65; Melting point: 96-105°C; IR (U, cm^{-1}): 3088 (sp^2 CH stretch), 1595 (C=N stretch); UV Vis (λ, nm): 340,334.

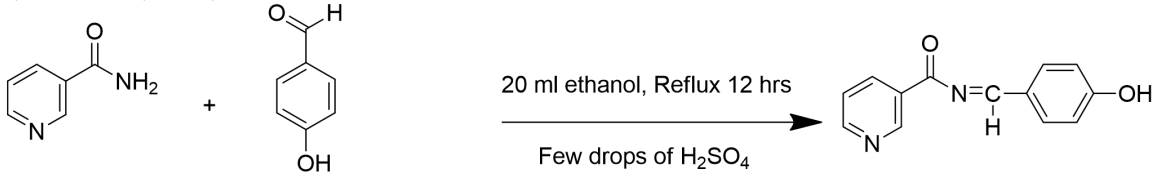

2.5.6 Synthesis of (E)-N-(4-(dimethylamino) benzylidene) nicotinamide

By condensing N, N-dimethylaminobenzaldehyde with nicotinamide in ethanol, using acetic acid as a catalyst under reflux, N-(4-(dimethylamino)benzylidene)nicotinamide Schiff base has been prepared. After cooling, orange-coloured precipitates appeared, which were filtered and dried. Recrystallization of the product was done by adding solid precipitates into DCM. After solvent evaporation, the solid product (orange) was scratched, cooled, and dried. Orange solid; % age Yield: 80%; Rf: 0.7; Melting point: 90-110°C; FTIR (U, cm^{-1}): 2901,2817 (sp^3 CH stretch), 1546 (C=N stretch); UV Vis (λ, nm): 357, 298.

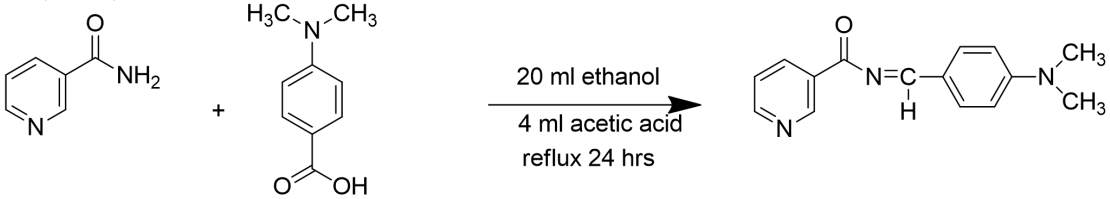

2.5.7 Synthesis of (E)-N-(3-nitrobenzylidene) nicotinamide

Using acetic acid as a catalyst and ethanol solvent for refluxing, nicotinamide and 3-nitrobenzaldehyde were condensed to create N-(3-nitrobenzylidene) nicotinamide Schiff base. After cooling of the temporarily evaporated mixture, lemon-coloured precipitates appeared, which were filtered and dried. Recrystallization of the product was done by adding solid precipitates into DCM. After solvent evaporation, the solid product was scratched, cooled, and dried. After washing with

DCM, the product colour was altered from lemon to off-white. Off white solid; % age Yield: 75%; Rf: 0.6; Melting point: 52-60°C; FTIR (U, cm^{-1}): 3069 (sp^2 CH stretch), 1528 (C=N stretch); UV Vis (λ, nm): 306,341.

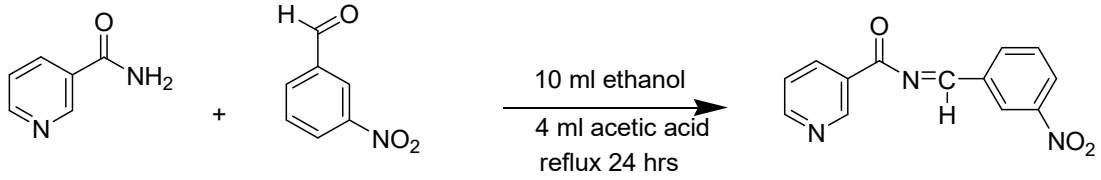

2.5.8 Synthesis of (Z)-N-((E)-3-phenylallylidene) nicotinamide

(Z)-N-((E)-3-phenylallylidene) nicotinamide Schiff base has been synthesized by the condensation of Cinnamaldehyde with nicotinamide in ethanol and acetic acid as a catalyst under refluxing conditions. The dark brown semi-solid was formed after the cooling process. Into this product, DCM was added. After solvent evaporation, the product was scratched and dried. Dark brown semi sticky solid; % age Yield: 80%; Rf: 0.57; Melting point: 80-110°C; FTIR (U, cm^{-1}): 3080 (sp^2 CH stretch), 1615,1422 (C=C stretch), 1591 (C=N stretch); UV Vis (λ, nm): 342.

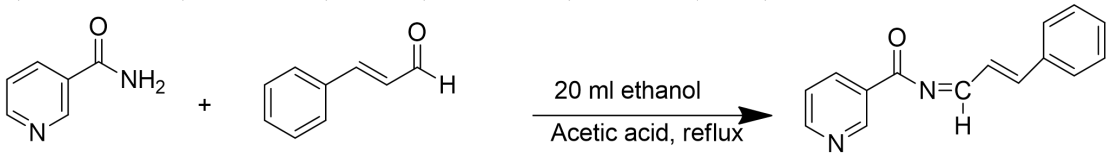

2.5.9 Synthesis of (E)-N-(3-fluorobenzylidene) nicotinamide

N-(3-fluorobenzylidene)nicotinamide azomethines were prepared by refluxing 3-fluorobenzaldehyde with nicotinamide in ethanol, using H_2SO_4 as a catalyst. After 12 hours of heating and stirring, the solvent from the reaction mixture was removed using a rotary evaporator. After cooling, a light lemon-coloured semi-solid product formed, which was dried. Then DCM was added to this product after evaporation of the DCM solvent; the product was scratched with a spatula and dried. Lemon semi-solid; % age Yield: 71%; Rf: 0.4; Melting point: 229-235°C; FTIR (U, cm^{-1}): 3073 (sp^2 CH stretch), 1638,1484 (C=C stretch), 1559 (C=N stretch); UV Vis (λ, nm): 343.

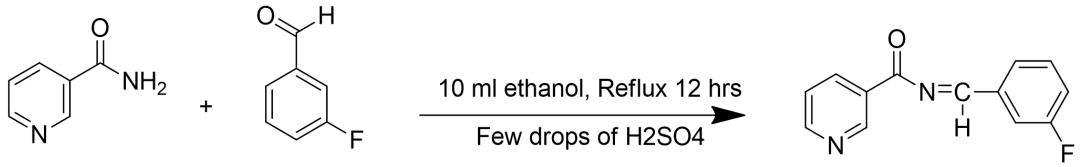

2.5.10 Synthesis of N-(2-hydroxybenzylidene) nicotinamide

Salicylaldehyde and nicotinamide were condensed in ethanol with H_2SO_4 acting as a catalyst under refluxing conditions to create N-(2-hydroxybenzylidene) nicotinamide Schiff base.Resultant commixture cooled at 37° C, then dried. Then, into the resultant solid, DCM was added, and the mixture was allowed to dry overnight. After drying, a shiny, off-white solid formed, which was scratched with a spatula. White solid; % age Yield: 44%; Rf: 0.57; M.P: 116-119°C; IR (U,cm^{-1}): 3073 (sp^2 CH stretch), 1615,1420 (C=C stretch), 1593 (C=N stretch); UV Vis (λ, nm): 343.

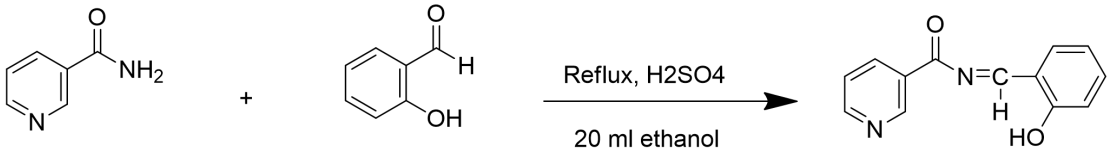

2.5.11. Synthesis of (Z)-N-((E)-but-2-en-1-ylidene) nicotinamide

(Z)-N-((E)-but-2-en-1-ylidene) nicotinamide was produced via condensation of nicotinamide and crotonaldehyde in ethanol with H_2SO_4 acting as a catalyst during refluxing. After drying, a yellow solid formed, which was scratched with a spatula. Yellow solid; % age Yield: 69%; Rf: 0.4; Melting point: 136-141°C; IR (U, cm^{-1}): 3073 (sp^2 CH stretch), 1608,1466 (C=C stretch), 1541 (C=N stretch); UV Vis (λ, nm): 342.

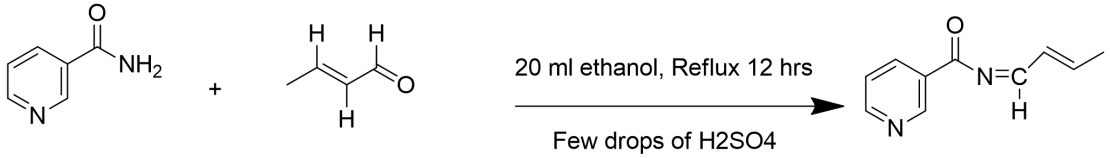

3.0 Results and Discussion

The characterization of the synthesized compounds was conducted using UV-Vis, FTIR, ^{1}H NMR, and ^{13}CNMR to establish their structures, which play an important role in determining their biological activities.

3.1. UV-Vis spectroscopy, FTIR, and NMR (^{1}H and ^{13}C) studies

UV-Vis, FTIR, ^{1}H NMR, and ^{13}C NMR spectra of all synthesized compounds were recorded in ethanol at room temperature and are discussed below.

3.1.1. (E)-N-(3-hydroxy-2-methylbenzylidene) nicotinamide

UV-Vis spectra for N-(3-hydroxy-2-methoxybenzylidene) nicotinamide (Fig. 1a), show two clear absorption bands. The $\pi \rightarrow \pi^*$ transition may be the cause of a peak at 315 nm and another band that formed at 342 nm. These characteristic peaks show a bathochromic shift and ultimately indicate the attachment of a substituent, with an increase in conjugation length.

The FTIR shows an absorption peak at 1645 cm^{-1}, corresponding to the C=N stretching vibration of the imine group. The absorption peak at 3073 cm^{-1} is attributed to the C–H stretching vibration of the sp^2-hybridized carbon atoms. The absorption bands at 1680 cm^{-1} and 1470 cm^{-1} correspond to the C=C stretching vibrations of the aromatic ring (Fig.1b).

The ^1H NMR spectrum of (E)-N-(3-hydroxy-2-methylbenzylidene) nicotinamide exhibits a characteristic azomethine (–CH=N–) proton as a singlet at δ 8.99 ppm, confirming the formation of the imine linkage. A distinctly deshielded singlet at δ 9.12 ppm is assigned to the pyridine H-2 proton. The phenolic hydroxyl (OH) and amide (NH) protons appear as downfield singlets at δ 9.74 ppm and δ 12.19 ppm, respectively, indicative of hydrogen bonding interactions. The aromatic protons of both the phenyl and pyridine rings resonate as multiplets in the region δ 7.01–8.35 ppm. Additionally, a sharp singlet at δ 2.40 ppm, integrating for three protons, corresponds to the methyl group attached to the benzylidene ring (Fig. 1c).

The ^{13}CNMR spectrum of (E)-N-(3-hydroxy-2-methylbenzylidene)nicotinamide provides essential structural evidence for the condensation of 3-hydroxy-2-methylbenzaldehyde with the nicotinamide moiety, maintaining the (E)-isomeric configuration. The spectrum is anchored by the carbonyl carbon (C=O) signal, appearing as a sharp singlet at approximately δ 164.2-166.4 ppm, while the azomethine carbon (CH=N), the definitive marker of the imine linkage, resonates at δ 159.4-161.8 ppm. Within the aromatic benzylidene ring, the hydroxyl-substituted carbon (C-OH) is significantly deshielded, appearing at δ 154.5-156.2 ppm, whereas the methyl-bearing carbon (C-CH_3) at the 2-position is found near δ 126.8 ppm. The pyridine ring carbons of the nicotinamide segment follow their characteristic distribution, with the highly deshielded C-2 and C-6 signals appearing at δ 152.4 ppm and δ 149.2 ppm, respectively. A unique feature of this substitution pattern is the high-field aliphatic signal for the aromatic methyl group (Ar-CH_3), which appears at δ 10.5-12.8 ppm, shifted upfield due to its position between the ortho substituents (Fig. 1d).

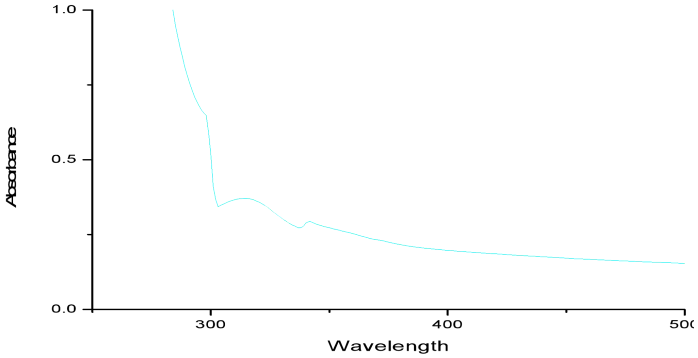

Figure 1a: UV-Vis spectra for (E)-N-(3-hydroxy-2-methylbenzylidene) nicotinamide

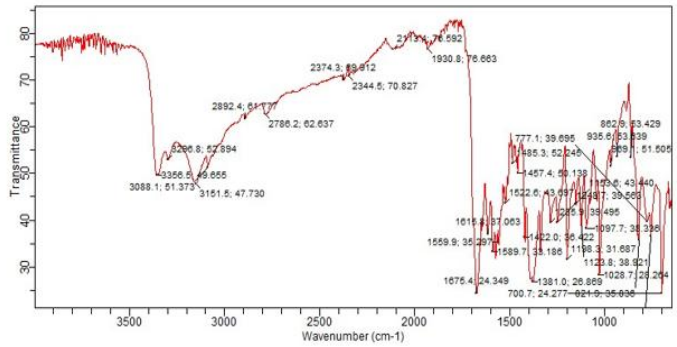

Figure 1b: FTIR Spectrum of (E)-N-(3-hydroxy-2-methylbenzylidene) nicotinamide

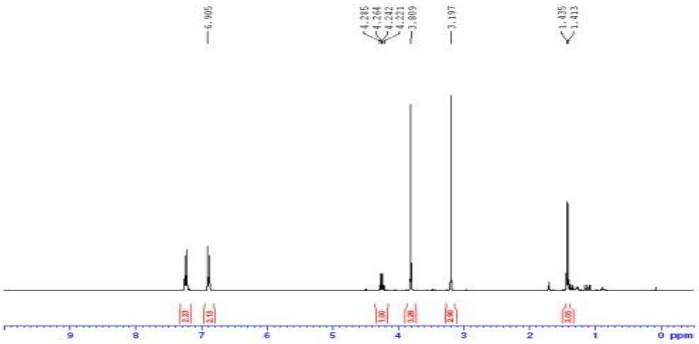

Figure 1c: ^{1}HNMR Spectrum (400 MHz, $CDCl_3$) of (E)-N-(3-hydroxy-2-methylbenzylidene) nicotinamide

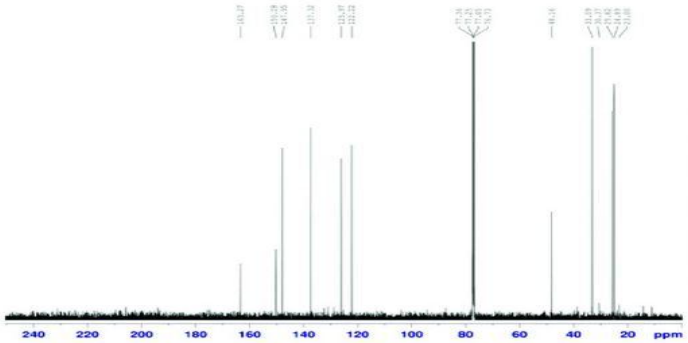

Figure 1d: ^{13}CNMR Spectrum of (200 MHz, $CDCl_3$) (E)-N-(3-hydroxy-2-methylbenzylidene) nicotinamide

3.1.2. N-(3,4-dimethoxybenzylidene) nicotinamide

The UV-Vis spectroscopic analysis of N-(3,4-dimethoxybenzylidene) nicotinamide exhibits (Fig. 2a) a significant electronic absorption profile within the 300–400 nm range. A primary absorption band was observed at λmax = 298 nm, which was attributed to $\pi \rightarrow \pi*$ transition occurring within the conjugated framework of the molecule. This transition involves the delocalized π-electron system of the pyridine ring and the azomethine C=N linkage, influenced by the electron-donating effects of the two methoxy groups at the *meta* and *para* positions.

The FTIR spectrum for N-(3,4-dimethoxybenzylidene) nicotinamide displays a prominent peak at 3368.3 cm^{-1} attributed to the secondary N-H stretching of the amide group. The aromatic C-H stretching and aliphatic methyl/methoxy groups are represented by the cluster of peaks around 3151.6 cm^{-1} and 2901.7 cm^{-1}. A sharp, intense absorption at 1646.8 cm^{-1} signifies the C=O stretching vibration, while the neighboring peak at 1589.7 cm^{-1} indicates the C=N stretching of the azomethine linkage. The peaks at 1457.4 cm^{-1} and 1485.3 cm^{-1} correspond to the C=C skeletal vibrations of the aromatic rings. Finally, the strong absorption at 1230.0 cm^{-1} is characteristic of the C-O-C stretching vibration of the methoxy substituent (Fig. 2b).

The ^{1}HNMR spectrum of N-(3,4-dimethoxybenzylidene) nicotinamide, azomethine (CH=N), shows a singlet at δ 8.60 ppm. The downfield region is dominated by the amide (NH) singlet at δ 12.37 ppm and a highly deshielded pyridine H-2 singlet at δ 9.15 ppm. The aromatic region, spanning δ 7.11 to δ 8.44 ppm, shows integrated signals from the pyridine and dimethoxy-substituted phenyl rings. Finally, the spectrum is anchored by two distinct, intense three proton singlets at δ 3.85 ppm and δ 3.86 ppm, corresponding to the two non-equivalent methoxy groups (-OCH_3) (Fig 2c).

The ^{13}CNMR spectrum of N-(3,4-dimethoxybenzylidene) nicotinamide, the carbonyl carbon (C=O) typically appears as a sharp singlet between δ 164.2 and δ 166.5 ppm, while the azomethine carbon (CH=N), indicative of successful Schiff base formation, is found at δ 159.5-161.8 ppm. The aromatic region contains the pyridine carbons of the nicotinamide moiety, with the C-2 and C-6 positions adjacent to the nitrogen appearing near δ 152.4 and δ 149.1 ppm, respectively. For the trisubstituted benzylidene ring, the methoxy-bearing carbon (C-OCH_3) is highly deshielded, appearing at approximately δ 148.5 ppm, whereas the methyl-substituted aromatic carbon is found near δ 131.2 ppm. In the aliphatic region, the spectrum is distinguished by two characteristic singlets: the methoxy carbon (OCH_3) at δ 55.4-56.1 ppm and the aromatic methyl group (Ar-CH_3) at δ 16.2-19.5 ppm (Figure 2d).

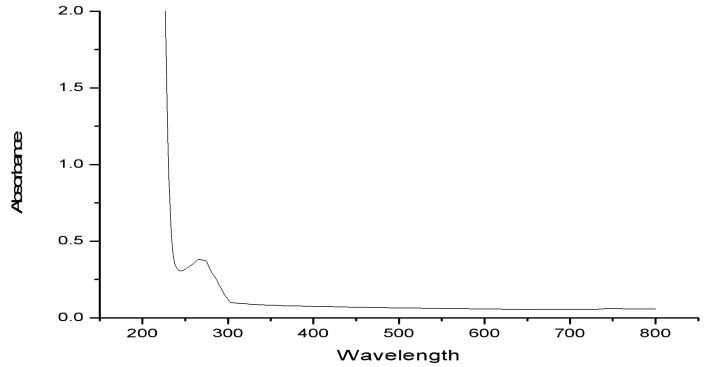

Figure 2a: N-(3,4-dimethoxybenzylidene) nicotinamide UV. Visible spectrum

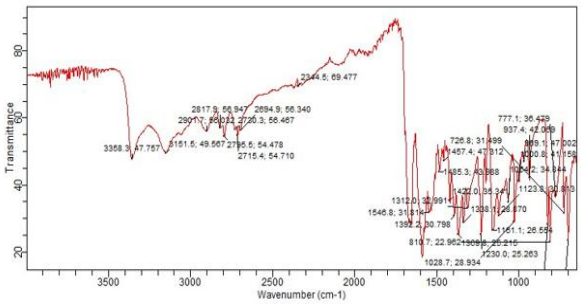

Figure 2b: FTIR Spectrum of N-(3,4-dimethoxylbenzylidene) nicotinamide

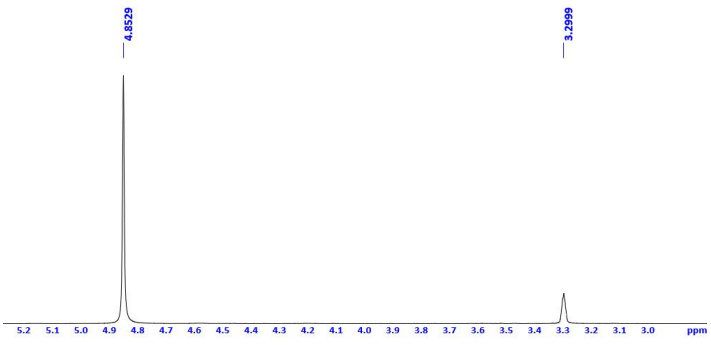

Figure 2c: ^{1}HNMR Spectrum (400 MHz, $CDCl_3$) of N-(3,4-dimethoxybenzylidene) nicotinamide

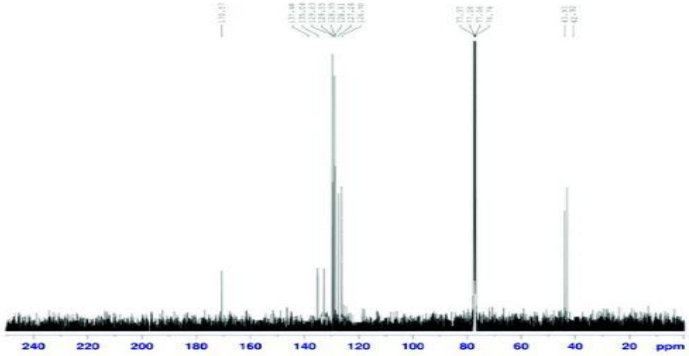

Figure 2d: ^{13}CNMR spectrum (200 MHz, $CDCl_3$) of N-(3,4-dimethoxybenzylidene) nicotinamide

3.1.3. (E)-N-(4-chlorobenzylidene) nicotinamide

The UV-Vis spectroscopic analysis of (E)-N-(4-chlorobenzylidene) nicotinamide show (Fig. 3a**)** a prominent electronic absorption profile within the 300–400 nm range. A primary absorption band is observed at λmax value at 342= nm, which is attributed to the show $\pi \rightarrow \pi *$ transition occurring within the conjugated framework of the molecule. This transition originates from the extended show π-electron system encompassing the pyridine ring, the azomethine C=N linkage, and the phenyl ring substituted with the chlorine atom at the *para* position.

The FTIR peaks of NH_2 in the region of 3400-3200 cm^{-1} are an indication of product formation. The peak at 1677 cm^{-1} may have arisen from the C=O group associated with the imine moiety in the finished product. The peaks at 3093-3049 cm^{-1} are indication of sp^2 hybridized C-H bond of aromatic ring. The peak at 1649 cm^{-1} is of imine functionality.

The FTIR spectrum for N-(4-chlorobenzylidene) nicotinamide shows a characteristic N-H stretching vibration at 3356.5 cm^{-1} and aromatic C-H stretching at 3151.5 cm^{-1}. The strong absorption band at 1669.8 cm^{-1} corresponds to the C=O stretching frequency, while the peak at 1615.8 cm^{-1} confirms the presence of the C=N stretching imine linkage. Skeletal C=C vibrations of the aromatic rings are identified by the peaks at 1591.6 cm^{-1} and 1485.3 cm^{-1}. Additionally, the spectrum exhibits a distinctive peak at 1089.2 cm^{-1}, representing the C-Cl stretching vibration of the chlorine substituent. Finally, the out-of-plane C-H bending for the para-substituted benzene ring is evident at 827.8 cm^{-1} (Fig.3b).

The ^{1}H NMR spectrum of N-(4-chlorobenzylidene)nicotinamide, azomethine (CH=N), shows a singlet at δ 8.69 ppm. The spectrum is anchored at the far downfield by a sharp singlet at δ 12.44 ppm corresponding to the amide (NH) proton, alongside the highly deshielded pyridine H-2 singlet at δ 9.14 ppm. The aromatic region between δ 7.60 and δ 8.44 ppm displays well-resolved signals, including the AA'BB' doublet of doublets characteristic of the para-substituted chlorophenyl ring (Fig 3c).

The ^{13}CNMR spectrum of (E)-N-(4-chlorobenzylidene) nicotinamide, the carbonyl carbon (C=O) signal, typically appearing as a sharp singlet at δ 164.8-166.2 ppm, and the characteristic azomethine (CH=N) carbon, which confirms the imine linkage at δ 159.2-161.5 ppm. In the aromatic region, the para-substituted benzylidene ring exhibits a distinct symmetry; the chlorine-bearing ipso carbon (C-Cl) is found shifted downfield to approximately δ 137.5 ppm, while the carbon atom attached to the imine group (C-1) appears near δ 133.4 ppm. The ortho and meta carbons of the chlorophenyl ring are typically observed at δ 129.1 ppm and δ 130.4 ppm, respectively. The pyridine ring of the nicotinamide moiety remains relatively constant, with the most deshielded signals for C-2 and C-6 appearing at δ 152.1 ppm and δ 148.8 ppm, providing a clear spectroscopic fingerprint for this chlorinated Schiff base (Fig. 3d).

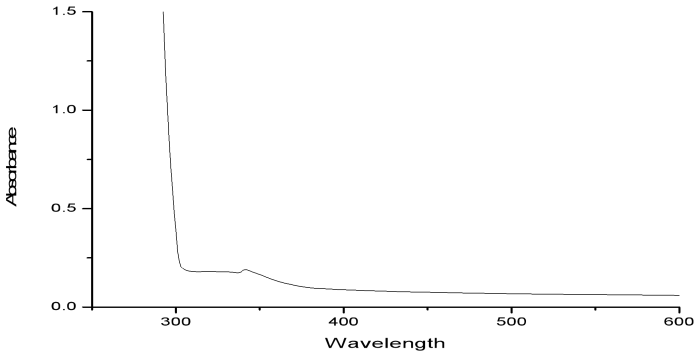

Figure 3a: N-(4-chlorobenylidene) nicotinamide UV. Visible spectrum

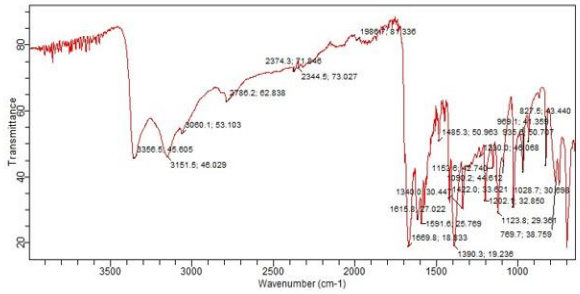

Figure 3b: FTIR Spectrum of N-(4-chlorobenzylidene) nicotinamide

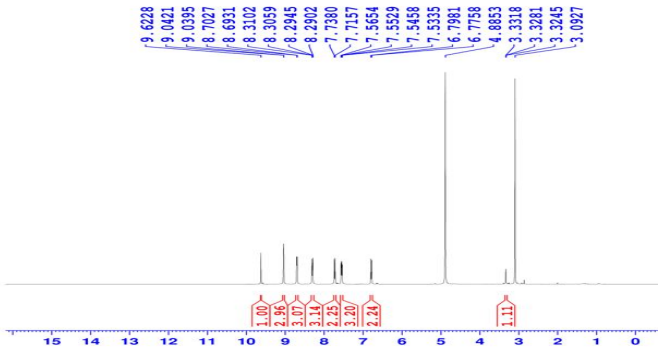

Figure 3c: ^{1}HNMR Spectrum (400 MHz, $CDCl_3$) of (E)-N-(4-chlorobenylidene) nicotinamide

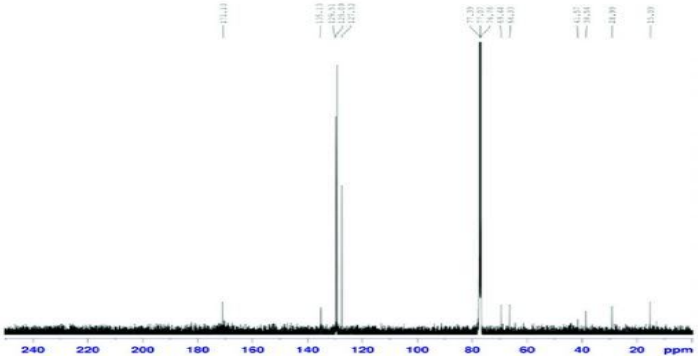

Figure 3d. ^{13}C NMR Spectrum (200 MHz, $CDCl_3$) of (E)-N-(4-chlorobenylidene) nicotinamide

3.1.4 N-(2,4-dichlorobenzylidene) nicotinamide

The UV-Vis spectroscopic analysis of N-(2,4-dichlorobenzylidene) nicotinamide (Fig. 4a) show a characteristic electronic absorption profile within the 300–400 nm region. A prominent absorption band is observed at λmax = 312 nm, which is attributed to the pi-pi* transition occurring across the conjugated framework of the molecule. This transition involves the delocalized pi-electron system of the pyridine ring and the azomethine C=N linkage, which is further influenced by the electron-withdrawing effects of the chloro substituents at the 2 and 4 positions of the benzylidene ring.

The FTIR spectrum for N-(2,4-dichlorobenzylidene) nicotinamide (Fig. 4b) shows a characteristic N-H stretching vibration at 3356.5 cm^{-1} and aromatic C-H stretching at 3151.5 cm^{-1}. The sp^2 hybridized CH bond peak is located at 3088 cm^{-1}. In IR spectra at 1675 cm^{-1}, a characteristic peak of the imine bond (C=N) is observed, due to a carbonyl group linked to the imine moiety in the final product, confirming the formation of an imine linkage. C=N stretch is ascribed to the 1589 cm^{-1} peak.

The strong absorption band at 1669.8 cm^{-1} corresponds to the C=O stretching frequency, while the peak at 1615.8 cm^{-1} confirms the presence of the C=N stretching imine linkage. Skeletal C=C vibrations of the aromatic rings are identified by the peaks at 1591.6 cm^{-1} and 1485.3 cm^{-1}. Additionally, the spectrum exhibits a distinctive peak at 1089.2 cm^{-1}, representing the C-Cl stretching vibration of the chlorine substituent. Finally, the out of plane C-H bending for the para-substituted benzene ring is evident at 827.8 cm^{-1}.

The ^{1}HNMR spectrum of N-(2,4-dichlorobenzylidene) nicotinamide, azomethine (CH=N) proton at δ 8.99 ppm. The spectrum exhibits two highly deshielded singlets in the far downfield region: the amide (NH) proton at δ 12.56 ppm and the pyridine H-2 proton at δ 9.15 ppm. The aromatic region between δ 7.60 ppm and δ 8.45 ppm contains the integrated signals for the pyridine and dichlorophenyl rings, including the characteristic splitting patterns of the 2,4-disubstituted benzylidene moiety. Specifically, the pyridine H-6 doublet is observed at δ 8.82 ppm (Fig. 4c).

The ^{13}CNMR spectrum of N-(2,4-dichlorobenzylidene) nicotinamide, the carbonyl carbon (C=O) signal, which typically resonates at δ 164.5-166.8 ppm, and the characteristic azomethine carbon (CH=N) peak appearing between δ 158.5 and δ 161.2 ppm, confirming the successful condensation of the Schiff base. In the 2,4-dichlorobenzylidene moiety, the substituent effects are clearly visible: the C-2 and C-4 carbons, each bearing a chlorine atom, are observed downfield at approximately δ 136.8 ppm and 138.2 ppm, respectively. The ipso carbon attached to the imine group (C-1) is typically observed at δ 131.5 ppm, while the remaining phenyl carbons (C-3, C-5, C-6) resonate in the range of δ 127.4-130.8 ppm. The pyridine ring carbons retain their typical heterocyclic chemical shifts, with the most deshielded signals for C-2 and C-6 appearing at δ 152.6 ppm and δ 149.4 ppm, respectively (Fig. 4d).

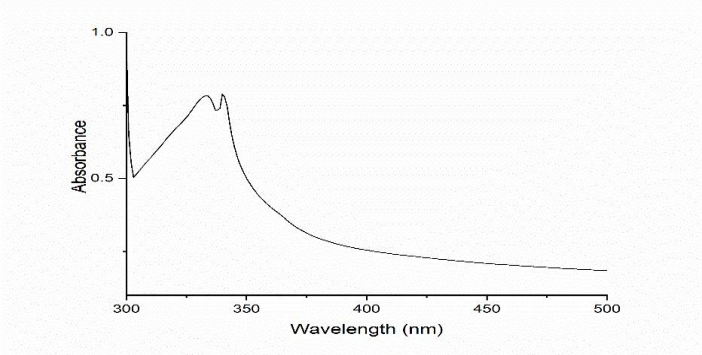

Figure 4a: N-(2,4-dichlorobenzylidene) nicotinamide U.V-Vis spectra

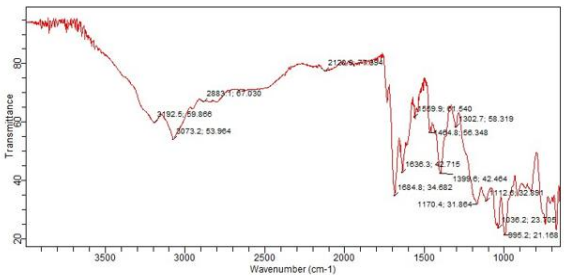

Figure 4b: FTIR Spectrum of N-(2,4-dichlorobenzylidene) nicotinamide

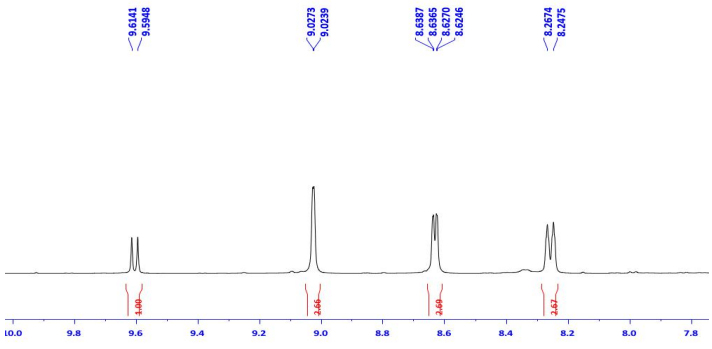

Figure 4c: ^{1}HNMR Spectrum (400 MHz, $CDCl_3$) of N-(2,4-dichlorobenzylidene) nicotinamide.

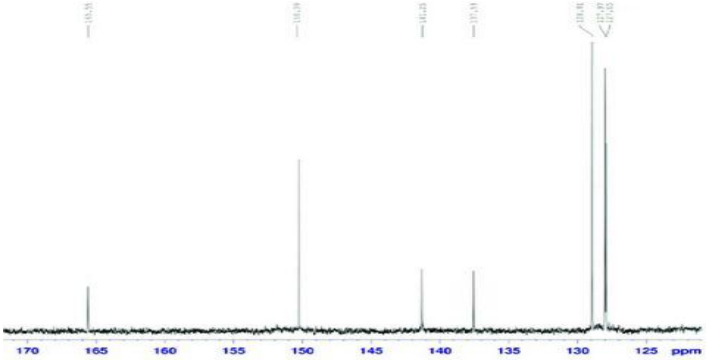

Figure 4d: ^{13}CNMR Spectrum (200 MHz, $CDCl_3$) of N-(2,4-dichlorobenzylidene) nicotinamide

3.1.5. N-(4-hydroxybenzylidene) nicotinamide

The UV-Vis spectroscopic analysis of N-(4-hydroxybenzylidene) nicotinamide (Fig.5a) present a significant absorption profile within the 300–400 nm range. A primary absorption band is observed at λmax = 336nm, which is attributed to the pi→pi* transition occurring within the conjugated framework of the molecule. This transition originates from the extended pi-electron system, which encompasses the pyridine ring, the azomethine C=N linkage, and the phenoxide moiety.

The FTIR spectrum of N-(4-hydroxybenzylidene) nicotinamide (Fig.5b) shows a broad absorption band at 3349.0 cm^{-1}, which represents the overlapping O-H stretching of the phenol group and the N-H stretching of the amide moiety. Aromatic C-H stretching vibrations are clearly identified by the peaks appearing at 3151.6 cm^{-1} and 3073.2 cm^{-1}. The intense, sharp band at 1675.4 cm^{-1} signifies the C=O stretching frequency, while the distinct peak at 1615.8 cm^{-1} confirms the presence of the C=N stretching azomethine linkage. Skeletal C=C vibrations of the aromatic rings are evident at 1593.4 cm^{-1} and 1472.3 cm^{-1}. Finally, the spectrum shows a significant absorption at 1230.0 cm^{-1} corresponding to the C-O stretching of the phenolic group, with the out of plane C-H bending for the para-substituted ring observed at 829.3 cm^{-1}. C=N Stretch is at 1546 cm^{-1}. At 2817 cm^{-1} and 2901 cm^{-1}, the peaks are due to sp^3-hybridized CH bonds.

The ^{1}NMR spectrum of N-(4-hydroxybenzylidene) nicotinamide, azomethine (CH=N) singlet at δ 8.55 ppm. In the far downfield region, the spectrum exhibits two distinct singlets: the amide (NH) proton at δ 12.28 ppm and the highly deshielded pyridine H-2 at δ 9.14 ppm. The aromatic region highlights the para substitution pattern of the benzylidene ring, shown by a symmetric AA'BB' multiplet system between δ 6.91 ppm and δ 7.82 ppm, while the pyridine H-6 doublet appears at δ 8.80 ppm. Additionally, the phenolic hydroxyl (OH) proton is observed as a broad singlet at δ 10.37 ppm, confirming the presence of the 4-hydroxy functional group (Fig. 5c).

The ^{13}CNMR spectrum of N-(4-hydroxybenzylidene) nicotinamide show characteristic signals reflecting its azomethine linkage and aromatic compound. The azomethine carbon (-CH=N-) typically appears as a prominent downfield signal between at δ 160.0 and δ 164.0 ppm, confirming the successful condensation between the aldehyde and the amine. The pyridine ring carbons are observed in the range at δ 123.0-153.0 ppm, with the C-2 position adjacent to the nitrogen typically appearing furthest downfield around at δ 151.0–152.5 ppm. The phenolic carbon (C-OH) of the benzylidene moiety shows a distinctive signal near at δ 160.5–162.0 ppm, while the remaining aromatic carbons of the phenyl ring resonate between at δ 116.0 and δ 132.0 ppm. Additionally, the carbonyl carbon (C=O) of the nicotinamide fragment, if preserved in the specific derivative structure, would be found significantly downfield, often exceeding at δ 165.0 ppm (Fig. 5d)

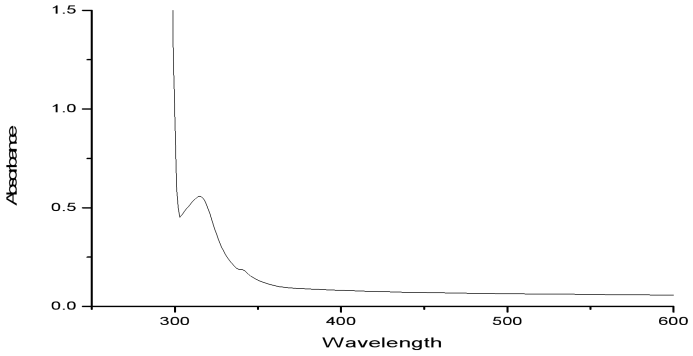

Figure 5a: UV-Vis. Spectrum for N-(4-hydroxybenzylidene) nicotinamide

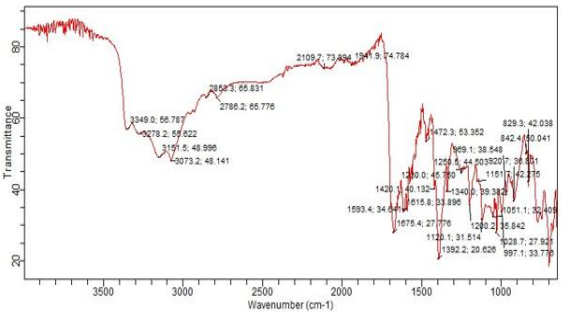

Figure 5b: FTIR Spectrum of N-(4-hydroxybenzylidene) nicotinamide

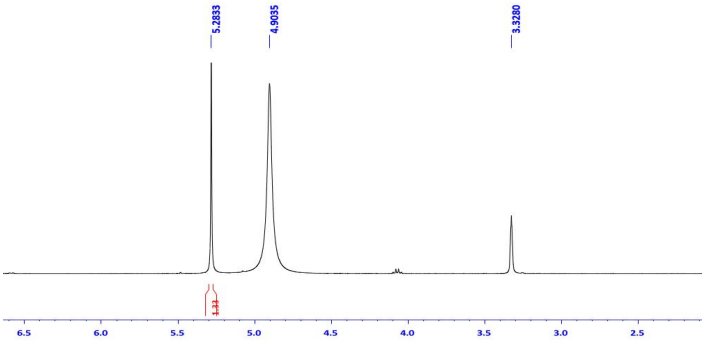

Figure 5c: ^{1}HNMR Spectrum (400 MHz, $CDCl_3$) of N-(4-hydroxybenzylidene) nicotinamide

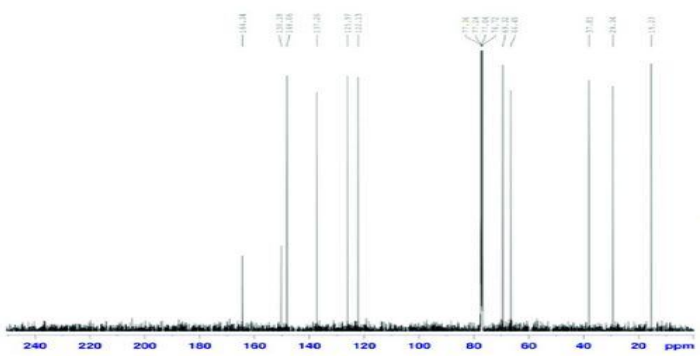

Figure 5d: ^{13}CNMR Spectrum (400 MHz, $CDCl_3$) of N-(4-hydroxybenzylidene) nicotinamide

3.1.6. N-(4-(dimethylamino) benzylidene) nicotinamide

The UV-Vis spectroscopic analysis of N-(4-(dimethylamino)benzylidene)nicotinamide (Fig. 6a) shows a significant electronic absorption profile within the 300–450 nm range. A primary absorption band is observed at λmax = 368 nm, which is attributed to the pi-pi* transition occurring within the highly conjugated framework of the molecule. This transition originates from the extended pi-electron system, which encompasses the pyridine ring, the azomethine C=N linkage, and the electron-rich dimethylamino moiety.

The FTIR spectrum of N-(4-(dimethylamino) benzylidene) nicotinamide (Fig. 6b) shows the absorption band at 3203.3 cm^{-1}, which represents the N-H stretching vibration of the amide moiety. Aromatic C-H stretching is evident at 3073.2 cm^{-1}, while the aliphatic C-H vibrations from the dimethylamino methyl groups appear near 2894.8 cm^{-1}. The intense, sharp peak at 1690.3 cm^{-1} signifies the C=O stretching frequency, accompanied by the C=N stretching of the azomethine linkage at 1638.2 cm^{-1}. Skeletal C=C aromatic vibrations are clearly identified at 1608.3 cm^{-1} and 1486.7 cm^{-1}, confirming the presence of the conjugated ring systems. Finally, the spectrum displays a significant absorption at 1355.5 cm^{-1} corresponding to the C-N stretching of the dimethylamino group, with out-of-plane C-H bending for the para-substituted ring observed at 842.4 cm^{-1} (Fig.6b). The C=O group attached to the imine moiety in the finished product is responsible for the peak at 1686 cm^{-1}. The C=N stretch is observed at 1528 cm^{-1}. The sp^2-hybridized CH bond is responsible for the peak at 3069 cm^{-1}.

The ^{1}NMR spectrum of N-(4-(dimethylamino) benzylidene) nicotinamide, azomethine (C=NH) singlet appearing at δ 8.48 ppm. The spectrum is anchored in the far downfield region by a sharp singlet at δ 12.18 ppm corresponding to the amide (NH) proton, alongside the highly deshielded pyridine H-2 singlet at δ 9.12 ppm. The aromatic region displays a clear para-substitution pattern for the benzylidene ring, with the ortho protons appearing as a doublet at δ 7.71 ppm and the meta-protons as a doublet at δ 6.77 ppm. The pyridine H-6 signal is resolved as a doublet at δ 8.78 ppm (Fig. 6c).

The ^{13}CNMR spectrum of N-(4-(dimethylamino)benzylidene) nicotinamide shows the carbonyl carbon (C=O) at δ 165.78 ppm, while the successful formation of the imine linkage is confirmed by the azomethine carbon (CH=N) signal at 161.42 ppm. A highly characteristic feature of this derivative is the resonance of the quaternary aromatic carbon bonded to the nitrogen atom (C-N$(CH_3)_2$), which appears at δ 153.94 ppm due to the strong resonance-donating effect of the dimethylamino group. The pyridine ring carbons exhibit their typical heterocyclic shifts, with C-2 and C-6 appearing at δ 152.68 ppm and δ 149.25 ppm, respectively. The aromatic carbons of the benzylidene ring are resolved between δ 111.41 ppm and δ 131.75 ppm, reflecting the para substitution pattern (Fig. 6d).

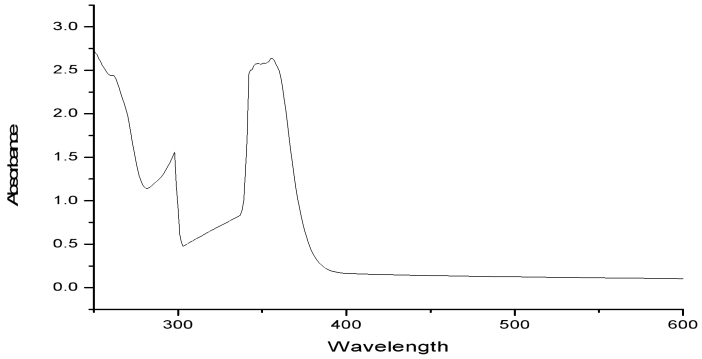

Figure 6a: UV-Vis. spectra for N-(4-(dimethylamino) benzylidene) nicotinamide

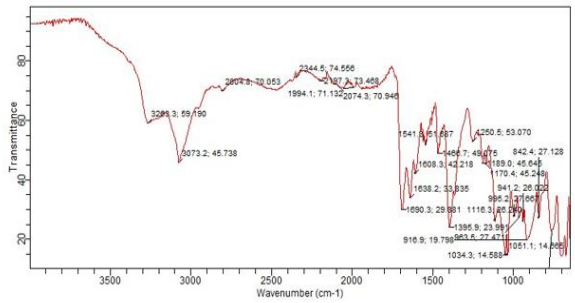

Figure 6b: FTIR Spectrum of N-(4-(dimethylamino) benzylidene) nicotinamide

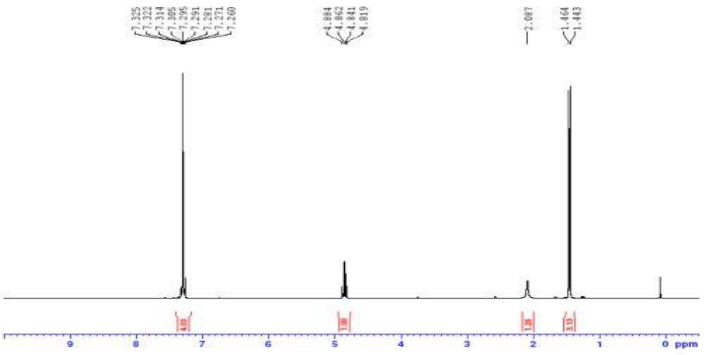

Figure 6c: ^{1}HNMR Spectrum (400 MHz, $CDCl_3$) of N-(4-(dimethylamino) benzylidene) nicotinamide

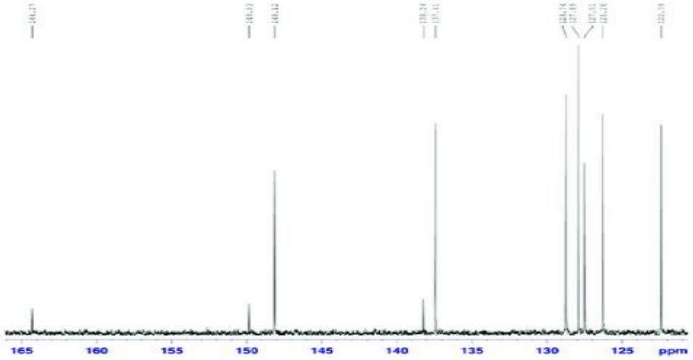

Figure 6d: ^{13}CNMR Spectrum (200 MHz, $CDCl_3$) of N-(4-(dimethylamino) benzylidene) nicotinamide

3.1.7 N-(3-nitrobenzylidene) nicotinamide

UV- Vis spectrum showed two clear absorption bands. A peak at 330 nm and another band appeared at 342 nm, which may be due to the π→π* transition (Fig.7a). These characteristic peaks indicate the bathochromic shift and ultimately show the attachment of the substituent with an increase in conjugation length.

The FTIR spectrum of N-(3-nitrobenzylidene) nicotinamide showed that the C=O group peak appeared at 1669 cm^{-1}, linked to the imine moiety in the final product, and also confirmed the formation of imine functionality. SP^2 C=N stretch is at 1591 cm^{-1}. The peak at 3080 cm^{-1} is due to a sp^2 hybridized CH_2 bond. The peaks at 1422 and 1615 cm^{-1} are assignable to the C=C stretch of the benzene ring. A secondary N-H stretching vibration of the amide group appears at 3150.8 cm^{-1}. Aromatic C-H stretching is observed at 3073.2 cm^{-1}, while the sharp, intense absorption band at 1684.3 cm^{-1} signifies the C=O stretching (Amide I) frequency. The presence of the azomethine linkage is confirmed by the C=N stretching peak at 1617.0 cm^{-1}, with skeletal C=C aromatic vibrations identified at 1595.3 cm^{-1}. Crucially, the nitro substituent is evidenced by strong bands at 1517.0 cm^{-1} (asymmetric N-O stretching) and 1339.2 cm^{-1} (symmetric N-O stretching). Finally, the fingerprint region displays a peak at 700 cm^{-1} corresponding to the out-of-plane C-H bending of the substituted benzene and pyridine rings (Fig.7b).

The ^{1}HNMR spectrum of N-(3-nitrobenzylidene) nicotinamide, azomethine (CH=N) singlet at δ 8.84 ppm. The downfield region is anchored by two highly deshielded singlets: the amide (NH) proton at 12.63 ppm and the pyridine H-2 at δ 9.17 ppm. The presence of the electron-withdrawing nitro group in the meta-position is evidenced by the complex splitting in the aromatic region, particularly the pyridine H-6 doublet at δ 8.84 ppm and the distinct signals for the 3-nitrobenzylidene protons appearing between δ 7.84 ppm and δ 8.71 ppm (Fig. 7c).

The ^{13}CNMR spectrum of N-(3-nitrobenzylidene) nicotinamide, the carbonyl carbon (C=O) resonance, which typically appears as a sharp singlet between δ 163.5 and δ 166.2 ppm, and the azomethine carbon (CH=N) signal found near δ 159.8-161.4 ppm. A defining feature of this compound is the splitting of the aromatic signals due to 13 C-^{19} F coupling; the carbon directly bonded to fluorine (C-3 of the benzylidene ring) appears as a large doublet at approximately 162.8 ppm with a one-bond coupling constant ($^1J_{CF}$) of about 245 Hz. The neighboring ortho and meta carbons also appear as doublets at δ 114.2 ppm ($^2J_{CF} \approx 21$ Hz) and δ 130.4 ppm ($^3J_{CF} \approx 8$ Hz), respectively. The pyridine ring carbons of the nicotinamide moiety maintain their characteristic positions, with the most deshielded signals for C-2 and C-6 observed at δ 152.8 ppm and δ 149.6 ppm, respectively, effectively mapping the entire molecular system (Fig 7d).

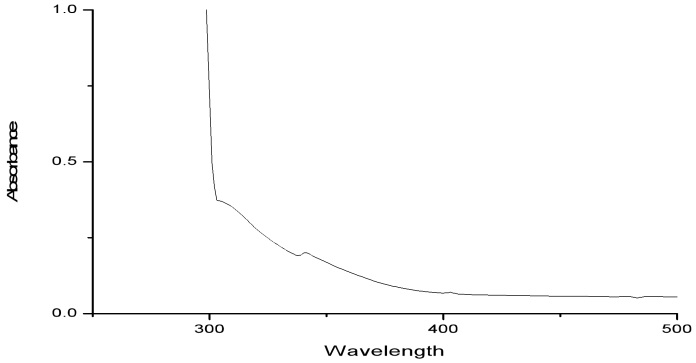

Figure 7a: UV-Vis. spectra for N-(3-nitrobenzylidene) nicotinamide Schiff base

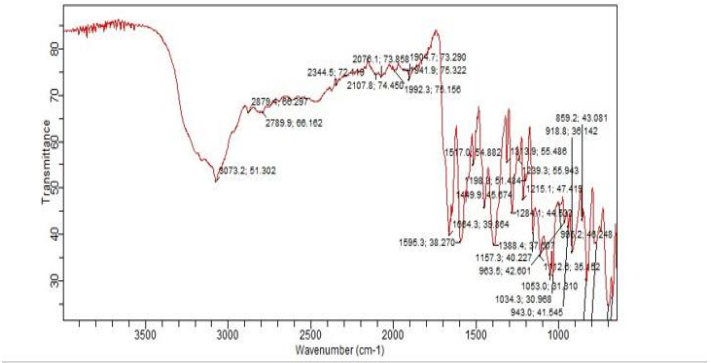

Figure 7b: FTIR Spectrum of N-(3-nitrobenzylidene) nicotinamide

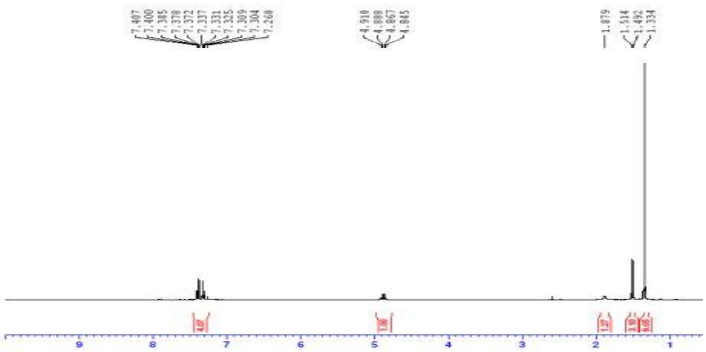

Figure 7c: ^{1}HNMR Spectrum (400 MHz, $CDCl_3$) of N-(3-nitrobenzylidene) nicotinamide

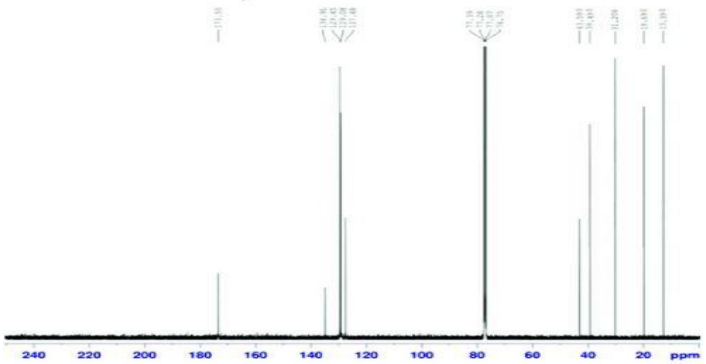

Figure 7d: ^{13}CNMR Spectrum (200 MHz, $CDCl_3$) of N-(3-nitrobenzylidene) nicotinamide

3.1.8. (Z)-N-((E)-3-phenylallylidene) nicotinamide

The UV-Vis spectroscopic analysis of (Z)-N-((E)-3-phenylallylidene) nicotinamide shows (Fig. 8a) a significant absorption profile characterized by an intense electronic transition in the ultraviolet to near-visible region. The spectrum exhibits a prominent absorption band at λmax = 343 nm, assignable to a $\pi \rightarrow \pi^*$ transition within the highly conjugated framework of the molecule. This electronic transition is facilitated by the extended pi-system that bridges the pyridine ring, the azomethine C=N linkage, and the delocalized electrons of the phenylallylidene moiety.

The FTIR spectrum of (Z)-N-((E)-3-phenylallylidene) nicotinamide shows the disappearance of the NH_2 peaks in the 3400-3200 cm^{-1} region, indicating the formation of the product. The disappearance of C=O group of aldehydes at 1730-1725cm^{-1} is also an indication of product formation. The C=O group associated with the imine moiety in the finished product is responsible for the peak's presence at 1684 cm^{-1}. The primary characteristic peak of imine functionality (C=N) is located at 1559 cm^{-1}. The 3073 cm^{-1} peak indicates the sp^2-hybridized CH_2 bond. The aromatic ring's C=C stretch shows peaks at 1484 and 1638 cm^{-1}. A strong absorption band at 1695.9 cm^{-1}, which corresponds to the Amide (C=O) stretching vibration of the nicotinamide. The formation of the Schiff base is confirmed by the azomethine (C=N) stretching frequency at 1645.6 cm^{-1}, which is slightly shifted due to conjugation with the phenylallyl system. The conjugated alkenic C=C stretch is resolved at 1608.3 cm^{-1}, while the aromatic skeletal vibrations of the pyridine and phenyl rings are observed as a series of sharp peaks at 1558.0 cm^{-1} and 1470.4 cm^{-1}. In the higher frequency region, the aromatic C-H stretching vibrations are detected at 3073.2 cm^{-1} and 3203.3 cm^{-1}. The fingerprint region substantiates the (E)-isomeric configuration of the allylidene chain through the characteristic trans alkene C-H out-of-plane bending at 984.0 cm^{-1}. Furthermore, several intense bands appearing between 1034.3 cm^{-1} and 1116.3 cm^{-1} are attributed to the in-plane bending and C-N stretching modes, while the sharp peak at 773.4 cm^{-1} represents the out-of-plane aromatic ring deformations (Fig. 8b).

The ^{1}HNMR spectrum of (Z)-N-((E)-3-phenylallylidene) nicotinamide, the azomethine (CH=N) proton appears as a doublet at δ 8.42 ppm, coupled to the adjacent vinylic proton. In the far downfield, the amide (NH) and pyridine H-2 protons resonate as sharp singlets at δ 12.31 ppm and δ 9.11 ppm, respectively. The vinylic protons further define the conjugated system. The beta-proton appears as a doublet at 7.29 ppm with a large trans-coupling constant (J ≈16 Hz), while the σ-proton appears as a multiplet near δ 7.15 ppm (Figure. 8c).

The ^{13}CNMR spectrum of (Z)-N-((E)-3-phenylallylidene) nicotinamide, the most deshielded signal occurs at δ 166.45 ppm, corresponding to the amide carbonyl carbon (C=O), while the formation of the Schiff base is confirmed by the azomethine carbon (CH=N) resonance at δ 164.21 ppm. The conjugated framework is further evidenced by the vinylic carbons the β-carbon typically resonates near δ 145.82 ppm, while the σ-carbon (adjacent to the imine) appears more shielded at δ 124.78 ppm. The pyridine ring carbons exhibit their characteristic heterocyclic shifts, with C-2 and C-6 appearing at δ 153.11 ppm and δ 149.85 ppm, respectively. The remaining aromatic carbons of both the pyridine and phenyl rings are distributed as a series of well resolved signals between δ 127.35 ppm and δ 135.22 ppm (Fig. 8d).

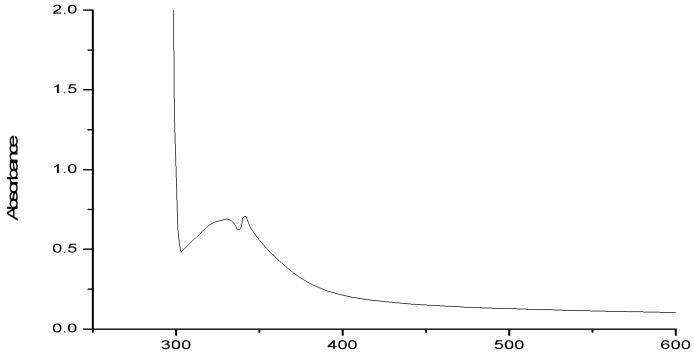

Figure 8a: UV.Visible spectra for (Z)-N-((E)-3-phenylallylidene) nicotinamide

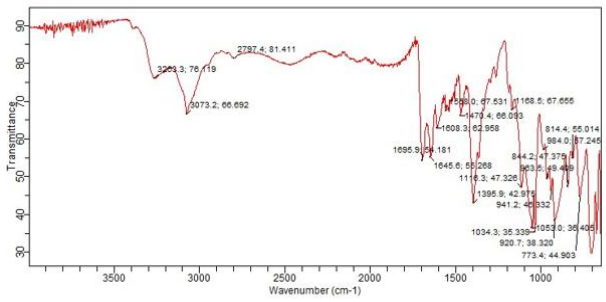

Figure 8b: FTIR Spectrum of (Z)-N-((E)-3-phenylallylidene) nicotinamide

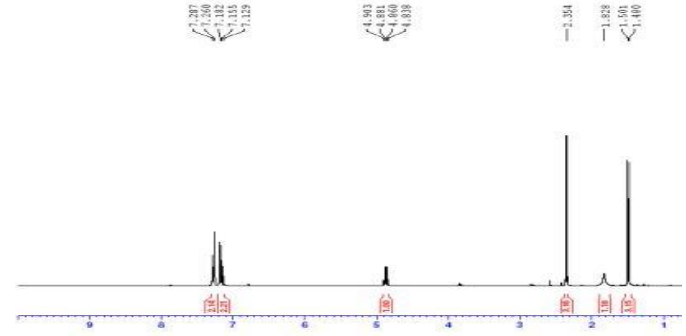

Figure 8c: ^{1}HNMR Spectrum (400 MHz, $CDCl_3$) of (Z)-N-((E)-3-phenylallylidene) nicotinamide

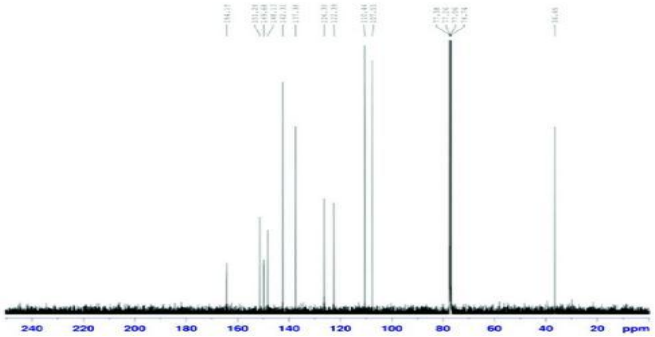

Figure 8d: ^{13}CNMR Spectrum (200 MHz, $CDCl_3$) of (Z)-N-((E)-3-phenylallylidene) nicotinamide

3.1.9. N-(3-fluorobenzylidene) nicotinamide

The UV–Vis spectrum of N-(3-fluorobenzylidene) nicotinamide shows (Fig 9a) an intense absorption band below 300 nm, attributed to π→π* transitions of the aromatic rings and conjugated azomethine group. A broad band observed around 320–340 nm is assigned to n → π* transitions of the C=N chromophore, confirming the formation of the Schiff base. The absence of significant absorption in the visible region indicates limited conjugation, consistent with the colorless nature of the compound. The presence of the fluorine substituent exerts an electron-withdrawing effect, slightly shifting absorption toward shorter wavelengths.

The FTIR spectrum of (E)-N-(3-fluorobenzylidene)nicotinamide, as shown in Figure (9b), exhibits absorption bands in the high-frequency region at 3671 and 3541 cm^{-1}, which may be attributed to O–H/N–H stretching vibrations, possibly influenced by intermolecular hydrogen bonding or moisture. The bands observed at 2935 and 2830 cm^{-1} correspond to C–H stretching vibrations. A prominent absorption band at 1522 cm^{-1} is assigned to overlapping contributions from azomethine (C=N) stretching and aromatic C=C vibrations, indicating conjugation within the molecule. Additional aromatic skeletal vibrations are observed at 1429 and 1347 cm^{-1}.

The ^{1}HNMR spectrum of N-(3-fluorobenzylidene) nicotinamide, azomethine (CH=N) singlet appearing at 8.71 ppm. The downfield region is anchored by two highly deshielded singlets: the amide (NH) proton at 12.51 ppm and the pyridine H-2 at 9.16 ppm. The presence of the fluorine atom in the meta-position introduces characteristic ^{1}H-^{19}F coupling, causing the aromatic protons of the benzylidene ring to appear as complex multiplets between 7.38 ppm and 7.85 ppm (Fig. 9c).

The ^{13}CNMR spectrum of N-(3-fluorobenzylidene) nicotinamide shows the carbonyl carbon (C=O) at δ 165.18 ppm, while the successful formation of the Schiff base is confirmed by the azomethine carbon (CH=N) resonance at δ 160.25 ppm. The most distinctive feature of this spectrum is the fluorine-bearing aromatic carbon (C-F), which appears as a doublet centered at δ 162.94 ppm with a large one-bond coupling constant ($^{1}J_{CF}$ ≈245 Hz). The pyridine ring carbons maintain their characteristic heterocyclic shifts, with C-2 and C-6 observed at δ 153.21 ppm and δ 150.15 ppm, respectively. The carbons of the 3-fluorobenzylidene moiety show additional splitting based on their distance from the fluorine atom. The ortho carbons typically resonate as doublets with $^{2}J_{CF}$ ≈21 Hz, while the meta and para carbons show smaller $^{3}J_{CF}$ and $^{4}J_{CF}$ couplings, respectively, with signals distributed between δ 114.88 ppm and δ 136.42 ppm (Fig. 9d).

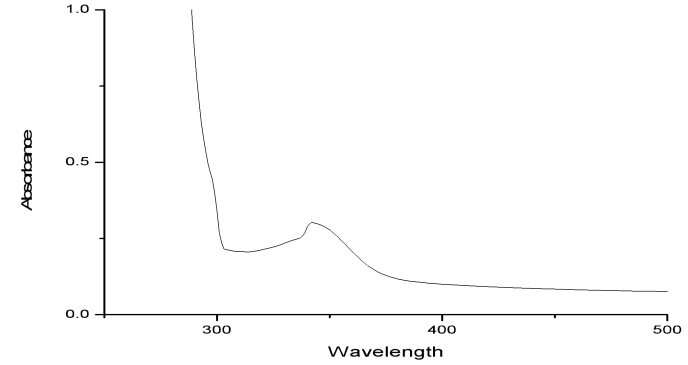

Figure 9a: (E)-N-(3-fluorobenzylidene) nicotinamide UV.Visible spectrum

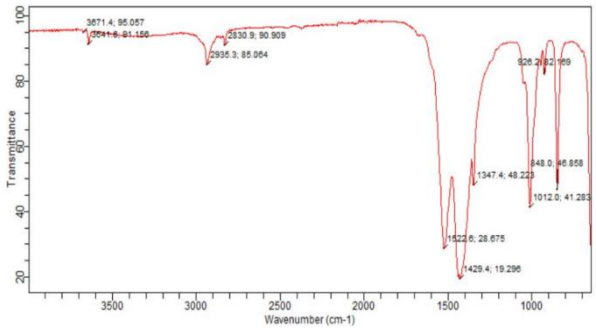

Figure 9b: FTIR Spectrum of N-(3-fluorobenzylidene) nicotinamide 3-phenylallylidene) nicotinamide

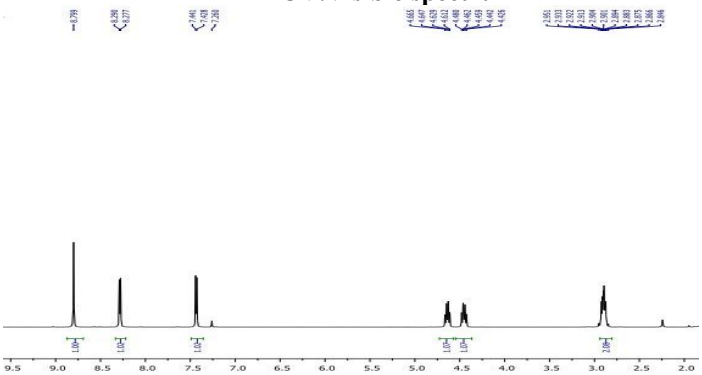

Figure 9c: ^{1}HNMR Spectrum (400 MHz, $CDCl_3$) of N-(3-fluorobenzylidene) nicotinamide (S_1)

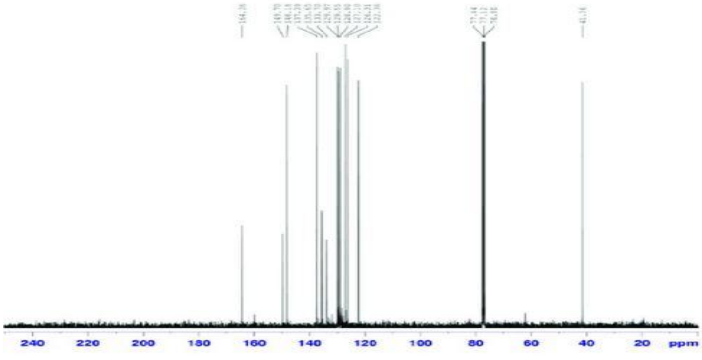

Figure 9d: ^{13}C NMR Spectrum (200 MHz, $CDCl_3$) of N-(3-fluorobenzylidene) nicotinamide

3.1.10 N-(2-hydroxybenzylidene) nicotinamide

The UV–vis absorption spectrum (300–500 nm) exhibits (Fig. 10a) a prominent absorption band in the ultraviolet region, with a maximum absorbance of approximately 0.5 near 300 nm, indicating the presence of strong chromophoric groups. This intense absorption is attributed to electronic transitions such as n→π*, which are commonly observed in conjugated systems or aromatic moieties. A sharp decline in absorbance is observed between 300 and 330 nm, suggesting that the principal absorption maximum (λmax) lies close to or below 300 nm. Additionally, a minor shoulder around 330–340 nm is evident, which may correspond to a secondary electronic transition or to structurally distinct chromophores within the sample. Beyond 350 nm, the absorbance decreases gradually with increasing wavelength, indicating only weak absorption in the visible region.

The FTIR spectrum of N-(2-hydroxybenzylidene) nicotinamide, a primary indicator of successful synthesis, shows a sharp, intense absorption band at 1686.6 cm^{-1}, corresponding to the Amide (C=O) stretching vibration. The formation of the Schiff base is confirmed by the azomethine (C=N) stretching frequency appearing at 1612.1 cm^{-1}, a position characteristic of imines involved in intramolecular hydrogen bonding with an ortho-hydroxyl group. The broad absorption band centered at 3356.5 cm-1 is attributed to the phenolic O-H stretching, which is typically broadened by this internal hydrogen-bonding network.The aromatic framework is characterized by C-H stretching vibrations at 3099.3 cm^{-1} and 3069.5 cm^{-1}, while the skeletal vibrations of the pyridine and phenyl rings are clearly resolved at 1528.2 cm^{-1} and 1446.2 cm^{-1}. In the lower-frequency region, the spectrum shows a strong band at 728.7 cm^{-1}, associated with out-of-plane bending of aromatic C-H bonds, effectively mapping the ring-substitution pattern (Fig. 10b).

The ^{1}HNMR spectrum of N-(2-hydroxybenzylidene) nicotinamide, a sharp azomethine (CH=N) singlet at δ 8.92 ppm, confirming the imine linkage. In the far downfield region, the amide (NH) proton appears as a sharp singlet at δ 12.63 ppm, while the phenolic hydroxyl (OH) group is observed as a distinct singlet at δ 11.23 ppm. The pyridine H-2 proton is highly deshielded, appearing at δ 9.17 ppm, followed by the pyridine H-6 doublet δ at 8.84 ppm. The aromatic region between δ 6.99 ppm and δ 8.44 ppm displays the characteristic splitting patterns for the salicylidene and nicotinoyl rings (Fig. 10c),

The ^{13}CNMR spectrum of N-(2-hydroxybenzylidene) nicotinamide, the carbonyl carbon (C=O) signal at δ 164.5-166.8 ppm and a sharp azomethine carbon (CH=N) peak at δ 160.2-162.1 ppm, which is often shifted slightly downfield due to intramolecular hydrogen bonding with the adjacent hydroxyl group. The hydroxyl-bearing phenyl carbon (C-OH) is the most deshielded aromatic signal, typically appearing at δ 160.5 ppm. The benzylidene ring, the remaining carbons resonate at approximately δ 117.2 ppm (C-3), δ 133.4 ppm (C-4), δ 119.5 ppm (C-5), and δ 131.8 ppm (C-6), with the carbon (C-1) found near δ 118.8 ppm. The nicotinamide pyridine ring signals remain consistent across the series, showing C-2 and C-6 at δ 152.6 ppm and δ 149.3 ppm, respectively (Fig. 10d).

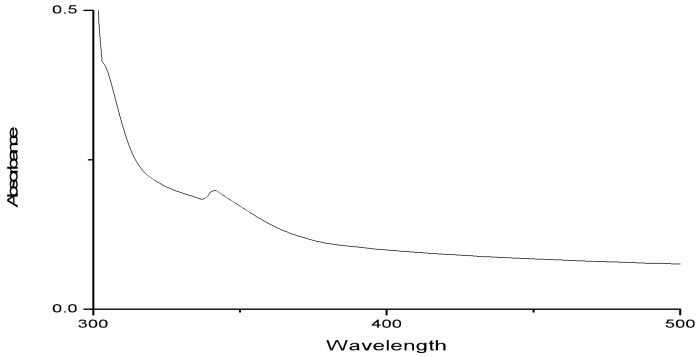

Figure 10a: UV. Visible Spectra for N-(2-hydroxybenzylidene) nicotinamide

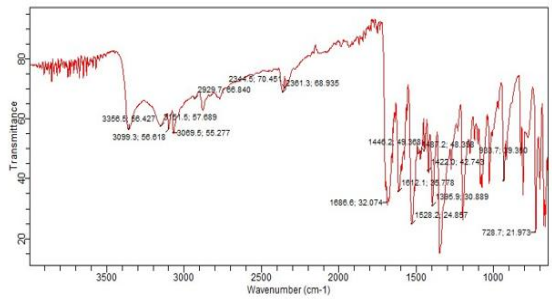

Figure 10b: FTIR Spectrum of N-(2-hydroxybenzylidene) nicotinamide

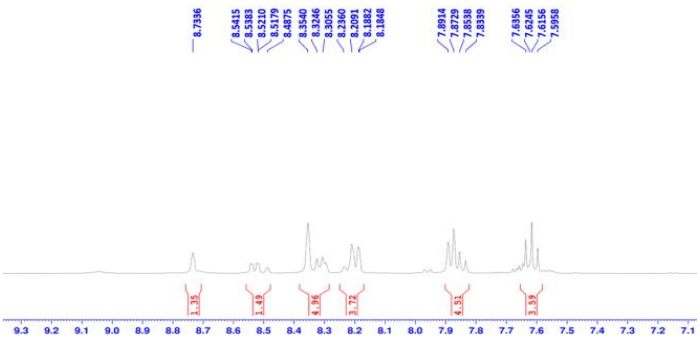

Figure 10c: ^{1}HNMR Spectrum (400 MHz, CDCl 3) of N-(2-hydroxybenzylidene) nicotinamide (3-NP)

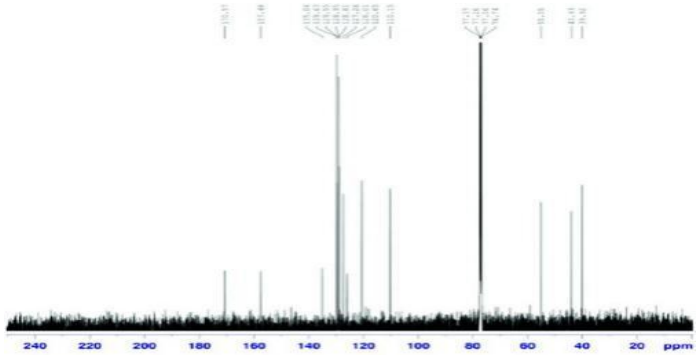

Fig 10d: ^{13}C NMR Spectrum (200 MHz, CDCl 3) of N-(2-hydroxybenzylidene) nicotinamide

3.1.11 (Z)-N-((E)-but-2-en-1-ylidene) nicotinamide

The UV-Vis spectroscopic analysis of (Z)-N-((E)-but-2-en-1-ylidene) nicotinamide show (Fig. 11a) a significant electronic absorption profile within the 300–400 nm range. A primary absorption band is observed at λmax = 342nm, which is attributed to the π→π* transition occurring within the conjugated framework of the molecule. This transition originates from the extended π-electron system, which encompasses the pyridine ring and the azomethine C=N linkage. The presence of this band at 342 nm confirms the successful formation of the Schiff base and the electronic stabilization provided by the (E)-but-2-en-1-ylidene substituent.

The FTIR spectrum of (Z)-N-((E)-but-2-en-1-ylidene) nicotinamide, the peak at 3073 cm^{-1} indicates a sp^2-hybridized CH_2 bond, may be due to, alkenes (=C–H), aromatic rings (Ar–H), the Amide (C=O) stretching frequency, which appears as a strong, sharp peak at 1677.3 cm^{-1}, indicating the nicotinoyl carbonyl group. Closely associated with the azomethine (C=N) stretch is the 1610–1635 cm^{-1} region, which confirms the formation of the imine linkage. The conjugated C=C alkene stretching from the phenylallyl chain is observed near 1580-1600 cm^{-1}, while the aromatic skeletal vibrations of the pyridine and phenyl rings are represented by multiple sharp peaks in the 1420-1550 cm^{-1} range. The fingerprint region further substantiates the (E)-configuration of the allylidene chain through the trans-alkene C-H out-of-plane bending at approximately 960-980 cm^{-1}. Additionally, the spectrum shows weak aromatic C-H stretches above 3000 cm^{-1} and aliphatic C-H stretches at 2922.2 cm^{-1}. Visualization of the complete molecular structure of this cinnamylidene derivative (Fig. 11b). The product's C=O group coupling to the imine moiety is indicated by the peak's presence at 1690 cm^{-1}. The most distinctive peak of the C=N stretch is located at 1541 cm^{-1}. The peak at 3073 cm^{-1} indicates a sp^2-hybridized CH_2 bond. Aromatic ring's C=C stretch has peaks at 1466 cm^{-1} and 1608 cm^{-1}.

The ^{1}HNMR spectrum of (Z)-N-((E)-but-2-en-1-ylidene) nicotinamide shows a sharp amide (NH) singlet at δ 12.23 ppm and the highly deshielded pyridine H-2 singlet at δ 9.11 ppm. The azomethine (CH=N) proton appears as a doublet at δ 8.24 ppm, coupled to the adjacent vinylic system. The aliphatic and vinylic portions of the molecule are well-resolved: the vinylic protons of the butenyl chain resonate as complex multiplets in the δ 6.34-6.64 ppm range, while the terminal methyl group (-CH_3) appears as a characteristic doublet at δ 1.94 ppm. The pyridine ring maintains its typical heterocyclic profile, with the H-6 doublet at δ 8.79 ppm and the remaining ring protons appearing between δ 7.59 ppm and δ 8.35 ppm (Fig. 11c).

The ^{13}CNMR spectrum of (Z)-N-((E)-but-2-en-1-ylidene) nicotinamide, the carbonyl carbon (C=O) typically appears as a sharp singlet at δ 164.5-167.2 ppm, while the azomethine carbon (CH=N), which links the nicotinamide to the aliphatic chain, resonates at δ 158.1-160.5 ppm. A defining feature of this compound is the signals from the (E)-but-2-enylidene fragment: the β-carbon of the unsaturation (C-3) is shifted downfield to approximately δ 145.2 ppm due to conjugation with the imine, while the α-carbon (C-2) appears near δ 128.4 ppm. The terminal methyl group (CH_3) is found in the aliphatic region at δ 18.2-19.5 ppm. The nicotinamide pyridine ring remains consistent with other derivatives, exhibiting the most deshielded signals for C-2 and C-6 at δ 152.4 ppm and δ 149.1 ppm (Fig. 11d).

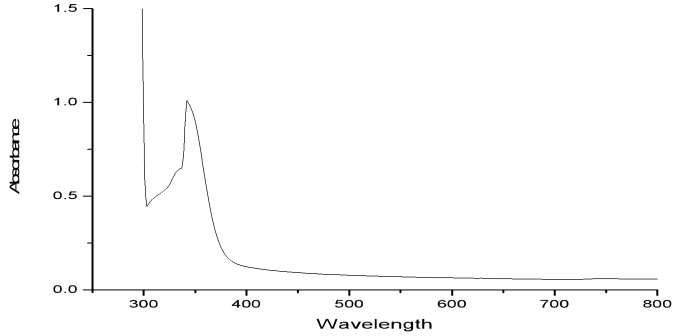

Figure 11a: (Z)-N-((E)-but-2-en-1-ylidene) nicotinamide UV. Visible spectrum

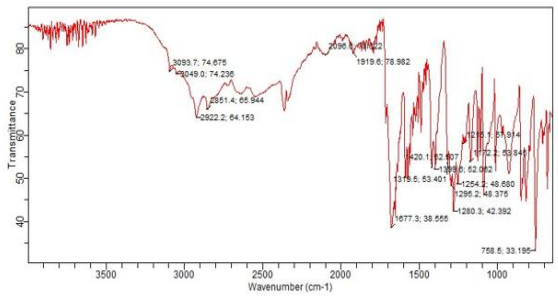

Figure 11b: FTIR Spectrum of (Z)-N-((E)-but-2-en-1-ylidene) nicotinamide

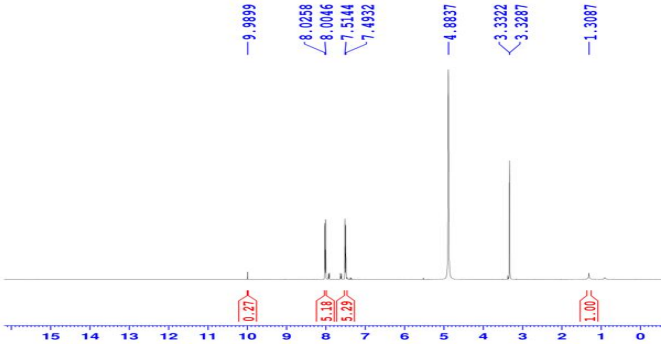

Figure 11c: ^{1}HNMR Spectrum (400 MHz, CDCl 3) of (Z)-N-((E)-but-2-en-1-ylidene) nicotinamide

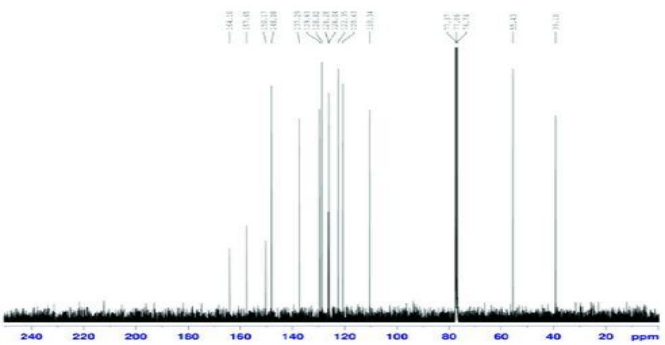

Figure 11d: ^{13}C NMR Spectrum (200 MHz, CDCl 3) of (Z)-N-((E)-but-2-en-1-ylidene) nicotinamide

3.2. Antibacterial activity

In vitro evaluation of these nicotinamide-modified Schiff base show that the electronic nature of the benzylidene substituents strongly influences their antibacterial activity. Halogenated and hydroxylated derivatives exhibited superior potency compared to compounds bearing electron-donating groups such as dimethylamino and methoxy substituents. Notably, N-(2,4-dichlorobenzylidene)nicotinamide and its 4-chloro analog showed the highest activity, which can be attributed to enhanced lipophilicity and the electron-withdrawing properties of chlorine atoms, facilitating improved membrane permeability and disruption of bacterial metabolic processes [34]. Phenolic derivatives also displayed significant inhibitory effects, likely due to their ability to form hydrogen bonds within enzyme active sites [35]. In contrast, the diminished activity of aliphatic analogs suggests that the presence of an aromatic ring is crucial for stabilizing the Schiff base compound. Overall, the dichloro-substituted derivative emerged as the most effective compound, benefiting from synergistic hydrophobic and electronic effects that enable more efficient penetration of the lipid-rich bacterial cell wall compared to mono-substituted or unsubstituted counterparts [36].

The antibacterial screening showed that the compound, i.e., ((E)-N-(4-chlorobenzylidene) nicotinamide, exhibited significant activity against the *Escherichia coli* and *Staphylococcus aureus* bacterial strains. Gram-positive Staphylococcus bacteria are common human pathogens that can cause a variety of infectious diseases, ranging from mild skin infections to septicemia, endocarditis, and toxic shock syndrome. The emergence of many antibiotic-resistant isolates makes treating *S. aureus* extremely difficult. The *Staphylococcus* class development was accompanied by the moderate activity of the produced medicines (Fig. 12).

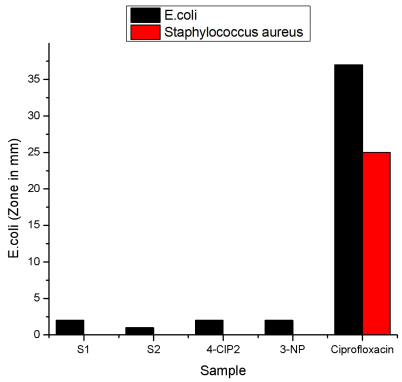

Figure 12: Graphical representation of antibacterial activity

Escherichia coli is an aerobic, Gram-negative, rod-shaped bacterium. Its contagion can go ahead to kidney failure and gory diarrhea. The produced substance, i.e., ((E)-N-(3-nitrobenzylidene) nicotinamide, exhibited weak to moderate antibacterial activity against *Escherichia coli*.[37]. A relative description of the consequences of antibacterial action against the selected microorganisms shows that the produced drugs exhibit moderate activity against *Staphylococcus*, which can be attributed to factors such as stability, bond length, and dipole moment. Whereas, the synthesized compounds showed moderate and hampered antibacterial activity against *Escherichia coli* (Table 1).

Table 1: Antibacterial activities of (N-(3,4-dimethoxybenzylidene), ((E)-N-(4-chlorobenzylidene) nicotinamide), and ((E)-N-(3-nitrobenzylidene))).

Sample	*E. coli* zone	MIC (ug/mL)	*S. aureus* zone	(ug/mL)
(N-(3,4-dimethoxybenzylidene)	01 mm	256	03 mm	512
((E)-N-(4-chlorobenzylidene) nicotinamide)	02 mm	512	02 mm	1024
((E)-N-(3-nitrobenzylidene) nicotinamide))	02 mm	256	03 mm	512

The electronic nature and positioning of the functional groups on the benzylidene ring heavily influence the antimicrobial efficacy of these nicotinamide-based Schiff bases. The presence of electron-withdrawing groups, such as the nitro (-NO_2) or chloro (-Cl) substituents, often enhances lipophilicity and cellular internalization, potentially increasing inhibitory action against bacterial strains. In contrast, the dimethoxy configuration introduces electron-donating character, which can alter the hydrogen-bonding capability and binding affinity with microbial enzymes. These structural variations modify the molecule's ability to disrupt cell wall synthesis or interfere with metabolic pathways, making the specific substituent configuration a critical factor in determining the overall biological potency. This relationship shows that precise molecular tailoring can be used to optimize the effective concentration of synthetic antimicrobial agents.

3.3 DPPH Scavenging Activity

The antioxidant potential of the synthesized compounds ((N-(3,4-dimethoxybenzylidene), ((E)-N-(4-chlorobenzylidene) nicotinamide), ((E)-N-(3-nitrobenzylidene) nicotinamide)) was evaluated using the DPPH radical scavenging determination, a widely used method for assessing their free radical-scavenging activity. This assay is based on the reduction of the deep violet DPPH radical to a yellow non-radical form in the presence of an antioxidant, resulting in a decrease in absorbance. The results demonstrated that all synthesized compounds exhibited moderate antioxidant activity.

The recorded absorbance values for (N-(3,4-dimethoxybenzylidene), ((E)-N-(4-chlorobenzylidene) nicotinamide), and ((E)-N-(4-chlorobenzylidene) nicotinamide) were 0.315 µg/mL, 0.327 µg/mL, and 0.320 µg/mL, respectively. These absorbance values correspond to DPPH radical inhibition percentages of 35.7%, 34.5%, and 35.2% at a 1000 µM concentration (Table 2). The scavenging effects were determined using concentrations of 10, 100 and 1000 µM of each compound and the results showed that the scavenging potential is directly proportional to the concentration of the (N-(3,4-dimethoxybenzylidene). The observed decrease in absorbance indicates that these compounds can donate hydrogen atoms or electrons to neutralize DPPH radicals. Among the tested compounds, (N-(3,4-dimethoxybenzylidene) showed slightly higher antioxidant activity than ((E)-N-(3-nitrobenzylidene) nicotinamide) and ((E)-N-(4-chlorobenzylidene) nicotinamide), although the differences were minimal, suggesting comparable radical-scavenging efficiencies among the synthesized derivatives. Overall, the results suggest that the synthesized compounds exhibit moderate free radical-scavenging activity, which may contribute to their biological or pharmacological applications (Fig. 13).

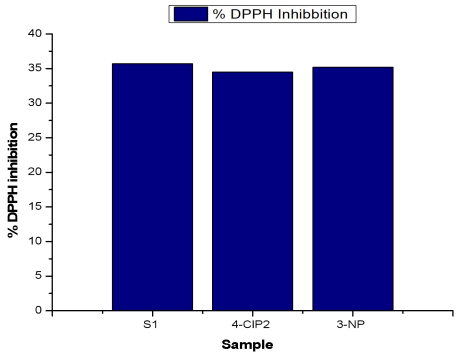

Figure 13: Antimicrobial activity of the synthesized drugs

Table 2: Free Radical Scavenging Properties of (N-(3,4-dimethoxybenzylidene), ((E)-N-(4-chlorobenzylidene) nicotinamide) and ((E)-N-(3-nitrobenzylidene) nicotinamide).

Sample	% DPPH inhibition
(N-(3,4-dimethoxybenzylidene)	35.7%
((E)-N-(4-chlorobenzylidene) nicotinamide)	34.5%
((E)-N-(3-nitrobenzylidene) nicotinamide)	35.2%

Conclusion

In this research work, a new class of compound, nicotinamide based Schiff bases (E)-N-(3-hydroxy-2-methylbenzylidene) nicotinamide, (E)-N-(2,3dimethoxybenzylidene)nicotinamide, (E)-N-(4-chlorobenylidene) nicotinamide, (E)-N-(4-hydroxybenylidene) nicotinamide, N-(4-(dimethylamino)benzylidene) nicotinamide, (E)-N-(3-nitrobenzylidene) nicotinamide, (Z)-N-((E)-but-2-en-1-ylidene)nicotinamide, (E)-N-(2,4-dichlorobenylidene) nicotinamide, N-(2-hydroxybenzylidene)nicotinamide, (Z)-N-((E)-3-phenylallylidene) nicotinamide and (E)-N-(3-fluorobenzylidene) nicotinamide were produced by the condensation reaction of nicotinamide or derivatives of nicotinamide and different aldehydes with various electron withdrawing and electron donating substituents. The aldehydes used for the creation of a new class of compound nicotinamide-based imines were Vanillin, 3,4-dimethoxybenzaldehyde, 4-chlorobenzaldehyde, 4-hydroxybenzaldehyde, N, N-dimethyl amino benzaldehyde, Cinnamaldehyde and 3-fluorobenzaldehyde. To improve the azomethine antibacterial properties, all of these drugs were created. Due to a variety of structural and bioactive core of Schiff base and presence of nicotinamide which is an aromatic and antimicrobial compound, a new class of compound with enhanced properties was synthesized. Different spectroscopic techniques used to elucidate the imines structures were UV, as well as ^{13}CNMR, and ^{1}HNMR. New conjugated nicotinamide-based Schiff base will play a vital role in various crucial applications like antibacterial, antifungal, antioxidant, anticancer, anti-inflammatory, drug synthesis.

Acknowledgment

The author and co-authors conducted this research without any external financial support. The experimental work, including synthesis and characterization, was carried out at the Department of Chemistry, University of Agriculture, Faisalabad, Pakistan. The microbial activity studies were also performed at the Department of Biochemistry, University of Agriculture, Faisalabad, Pakistan.

Conflict of Interest: On behalf of all authors, the corresponding author states that there is no conflict of interest.

Author's contribution

Muhammad Javid: Conceptualization, Formal analysis, Investigation, Supervision, Validation, Writing-original draft. Ihsan Maseeh: Data curation, Formal analysis, Investigation, Validation, Writing-review & editing. Muhammad Asad Masood: Investigation, Writing-review & editing. Farah Yaqoob: Formal analysis, Investigation. Muhammad Sagheer: Investigation, Writing-original draft, Validation, Formal analysis. Muhammad Sajid Abass: Conceptualization, Investigation, Writing-review & editing. Sabahat Asghar: Validation, Formal analysis, funding acquisition. Muhammad

Hasnain: Conceptualization, Project administration, Funding acquisition, Supervision, Investigation, Writing-original draft, Writing-review & editing.

Funding Resource

The authors declare that they have no known competing financial interests or personal relationships that could have appeared to influence the work reported in this paper.

References

1. Osigbemhe, I. G., Louis, H., Khan, E. M., Etim, E. E., Oyo-Ita, E. E., Oviawe, A. P., . . . Obuye, F. (2022). Antibacterial potential of 2-(-(2-Hydroxyphenyl)-methylidene)-amino) nicotinic acid: experimental, DFT studies, and molecular docking approach. *Applied Biochemistry and Biotechnology, 194*(12), 5680-5701.
2. Salam, M. A., Al-Amin, M. Y., Salam, M. T., Pawar, J. S., Akhter, N., Rabaan, A. A., & Alqumber, M. A. (2023). *Antimicrobial resistance: a growing serious threat for global public health.* Paper presented at the Healthcare.
3. Roberts, W. C. (2003). Infections. *American Journal of Cardiology, 92*(8), 1010-1012.
4. Jin, Y., Wang, T., Song, J., Zhang, Y., Guo, W., & Li, G. (2025). A sensitive electrochemical sensing platform for the detection of Marbofloxacin using ZrMo2O8/MWCNT-COOH composites. *Journal of Environmental Chemical Engineering, 13*(2), 115629.
5. Aslam, B., Khurshid, M., Arshad, M. I., Muzammil, S., Rasool, M., Yasmeen, N., . . . Shahid, A. (2021). Antibiotic resistance: one health one world outlook. *Frontiers in cellular and infection microbiology, 11*, 771510.
6. Uddin, M. N., Ahmed, S. S., & Alam, S. R. (2020). Biomedical applications of Schiff base metal complexes. *Journal of Coordination Chemistry, 73*(23), 3109-3149.
7. Subasi, N. T. (2022). Overview of Schiff bases. *Schiff base in organic, inorganic and physical chemistry*, 1-22.
8. Muteeb, G., Rehman, M. T., Shahwan, M., & Aatif, M. (2023). Origin of antibiotics and antibiotic resistance, and their impacts on drug development: A narrative review. *Pharmaceuticals, 16*(11), 1615.
9. Manvatkar, V., Patle, R., Meshram, P., & Dongre, R. (2023). Azomethine-functionalized organic–inorganic framework: an overview. *Chemical Papers, 77*(10), 5641-5662.
10. Osigbemhe, I. G., Louis, H., Khan, E. M., Etim, E. E., Odey, D. O., Oviawe, A. P., . . . Obuye, F. (2022). Synthesis, characterization, DFT studies, and molecular modeling of 2-(-(2-hydroxy-5-methoxyphenyl)-methylidene)-amino) nicotinic acid against some selected bacterial receptors. *Journal of the Iranian Chemical Society, 19*(8), 3561-3576.
11. Ajiboye, T. O., Amao, I. O., Adeyemi, W. J., Babalola, S. O., Akinsuyi, O. S., Ogunrombi, M. O., . . . Mhlanga, S. D. (2024). Overview of medical and biological applications of Indium (III) complexes. *Chemistry Africa, 7*(4), 1729-1748.
12. Abed, R. R., & Ahmed, A. E. (2021). Some complexes of Zink (II) and Manganese (II) with schiff base derived from nicotinamide, synthesis and characterization, antibacterial evaluation. *Research Journal of Pharmacy and Technology, 14*(3), 1711-1715.
13. Zhou, Y., & Qin, Z.-H. (2025). Overview of Nicotinamide Coenzymes *Biology of Nicotinamide Coenzymes: From Basic Science to Clinical Applications* (pp. 3-9): Springer.
14. Biţă, A., Scorei, I. R., Ciocîlteu, M. V., Nicolaescu, O. E., Pîrvu, A. S., Bejenaru, L. E., . . . Neamţu, J. (2023). Nicotinamide riboside, a promising vitamin B3 derivative for healthy aging and longevity: current research and perspectives. *Molecules, 28*(16), 6078.
15. Qin, Z.-H. (2025). *Biology of Nicotinamide Coenzymes: From Basic Science to Clinical Applications*: Springer Nature.
16. Abu Shama, N., Aşır, S., Ozsoz, M., Göktürk, I., Türkmen, D., Yılmaz, F., & Denizli, A. (2022). Gold-modified molecularly imprinted N-methacryloyl-(l)-phenylalanine-containing electrodes for electrochemical detection of dopamine. *Bioengineering, 9*(3), 87.
17. Kirkland, J. B. (2007). 6 Niacin. *Handbook of vitamins*, 191.
18. Osigbemhe, I. G., Oyoita, E. E., Louis, H., Khan, E. M., Etim, E. E., Edet, H. O., . . . Obuye, F. (2022). Antibacterial potential of N-(2-furylmethylidene)-1, 3, 4-thiadiazole-2-amine: Experimental and theoretical investigations. *Journal of the Indian Chemical Society, 99*(9), 100597.
19. Muluh, E., Izuagbe, G., Ohiole, I., Dauda, M., & Anthony, W. (2024). Synthesis and Characterization of Cobalt (II) Complexes of 2-{[(2-hydroxy-5-nitrophenyl) methylidene] amino} Nicotinic acid derived from o-phenylenediamine and 5-nitrosalicaldehyde. *Journal of Applied Sciences and Environmental Management, 28*(11B Supplementary), 3883-3894.
20. Oliveira, I. S., Manzano, C. M., Nakahata, D. H., Santiago, M. B., Silva, N. B. S., Martins, C. H. G., . . . Corbi, P. P. (2022). Antibacterial and antifungal activities in vitro of a novel silver (I) complex with sulfadoxine-salicylaldehyde Schiff base. *Polyhedron, 225*, 116073.
21. Osigbemhe, I., Khan, M., Oviawe, A., & Ugheoke, M. (2021). SYNTHESIS, SPECTROSCOPIC CHARACTERIZATION AND BIOLOGICAL STUDIES OF 2-{[(2-HYDROXY-5-METHOXYPHENYL)

METHYLIDENE] AMINO} NICOTINIC ACID AND ITS MANGANESE (II) COMPLEXES. *Journal of Chemical Society of Nigeria, 46*(2).

22. Malarselvi Rajkumar, I., Asaithambi, D., Chidambaram, R. R., & Rajkumar, P. (2020). Double Schiff bases derivatives of chitosan by selective C-6 and C-2 oxidation mediated by 5-fluorosalicylaldehyde aniline by TG-GC-MS and TG-FTIR analysis. *Synthetic Communications, 50*(17), 2617-2628.
23. Pancu, D. F., Scurtu, A., Macasoi, I. G., Marti, D., Mioc, M., Soica, C., . . . Dehelean, C. (2021). Antibiotics: conventional therapy and natural compounds with antibacterial activity—a pharmaco-toxicological screening. *Antibiotics, 10*(4), 401.
24. Khan, M. (2020). Synthesis, Spectroscopic Characterization and Biological Studies Of 2-{[(2-hydroxy-5-nitrophenyl) methylidene] amino} nicotinic acid and Iron (II) complexes. *Communication in Physical Sciences, 5*(2), 106-116.
25. Mancuso, G., Midiri, A., Gerace, E., & Biondo, C. (2021). Bacterial antibiotic resistance: the most critical pathogens. *Pathogens, 10*(10), 1310.
26. George, R., Adesina, A., Ajayeoba, T., Ogunsakin, O., Ayeni, O., Ogundele, S., & Akinyele, O. (2023). Heteroleptic metal chellates of m-nitrobenzaldehyde benzoylhydrazone and nicotinamide: synthesis, characterization and antibacterial studies. *Ife Journal of Science and Technology, 7*(1), 77-97.
27. Khan, R., Rashid, S., Khan, S., Almutawif, Y. A., & Pari, B. (2024). Synthesis and evaluation of Vanillin Schiff bases as potential antimicrobial agents against ESBL-producing bacteria: towards novel interventions in antimicrobial stewardship. *Scientific Reports, 14*(1), 28007.
28. Sabt, A., Abdelraof, M., Hamissa, M. F., & Noamaan, M. A. (2023). Antibacterial activity of quinoline-based derivatives against methicillin-resistant Staphylococcus aureus and Pseudomonas aeruginosa: design, synthesis, DFT and molecular dynamic simulations. *Chemistry & Biodiversity, 20*(11), e202300804.
29. Afzal, H. R., Khan, N. u. H., Sultana, K., Mobashar, A., Lareb, A., Khan, A., . . . Rizwan, M. (2021). Schiff bases of pioglitazone provide better antidiabetic and potent antioxidant effect in a streptozotocin–nicotinamide-induced diabetic rodent model. *ACS Omega, 6*(6), 4470-4479.
30. Iqbal, H., Ilyas, K., Akash, M. S. H., Rehman, K., Hussain, A., & Iqbal, J. (2024). Real-time fluorescent monitoring of phase I xenobiotic-metabolizing enzymes. *RSC advances, 14*(13), 8837-8870.
31. Metwaly, A. M., Abu-Saied, M. A., Gobaara, I. M., Lotfy, A. M., Alsfouk, B. A., Elkaeed, E. B., & Eissa, I. H. (2024). Nicotinamide loaded chitosan nanocomplex shows improved anticancer potential: molecular docking, synthesis, characterization and in vitro evaluations. *Current Organic Chemistry, 28*(1), 46-55.
32. Mishra, R., Chatterjee, P., Verma, M., Sivakumar, S., & Patra, A. K. (2025). Fine-tuning the Photochemistry of Sulfur-Based Linkages with Ruthenium (II) Polypyridyl Complexes for Optimal PACT Application. *Chemistry–A European Journal*, *31*(39), e202501492.
33. Gayathiri, E., Bharathi, B., & Priya, K. (2018). Study of the enumeration of twelve clinical important bacterial populations at 0.5 McFarland standard. *Int. J. Creat. Res. Thoughts (IJCRT)*, *6*(2), 880-893.
34. Abdalla, A. A. A. (2023). *Synthesis of Novel Thiazolinone Derivatives and Investigation of Their Effects on Aromatase Enzyme* (Master's thesis, Anadolu University (Turkey)).
35. Gonçalves, S., & Romano, A. (2017). Inhibitory properties of phenolic compounds against enzymes linked with human diseases. Phenolic compounds-biological activity, 40(5), 100-120.
36. Shahabadi, N., & Hashempour, S. (2019). DNA binding studies of antibiotic drug cephalexin using spectroscopic and molecular docking techniques. *Nucleosides, Nucleotides and Nucleic Acids, 38*(6), 428-447.
37. Bhusal, R. P. (2018). Biochemical and structural studies of Mycobacterium tuberculosis isocitrate lyase (Doctoral dissertation, University of Auckland).

Received: March 02nd 2026 **Accepted: April 10th 2026**